Title

Wood export varies among decadal, annual, seasonal, and daily scale hydrologic regimes in a large, Mediterranean climate, mountain river watershed

Authors

Senter, Anne E
Pasternack, Gregory B
Piegay, Herve
et al.

Publication Date

2016-10-01

DOI

10.1016/j.geomorph.2016.09.039

Wood export varies among decadal, annual, seasonal, and daily scale hydrologic regimes in a large, Mediterranean climate, mountain river watershed

Authors: Senter[1*], A.E., Pasternack[1], G.B., Piégay[2], H., Vaughan[1], M.C., Lehyan[1], J.S.

[1]Department of Land, Air, and Water Resources, University of California at Davis, Davis, CA 95616.

[2] Université of Lyon, CNRS, UMR 5600 - Environnement Ville Société, Site ENS of Lyon, France

* Corresponding author: aesenter@ucdavis.edu

Abstract

The dynamics that move wood through and out of watersheds are complex and not yet fully understood. In this study, climatic conditions, hydrologic responses, and watershed processes were explored to better understand variations in wood export using aerial imagery, event-based video monitoring, and field measurements from the 1097 km^2 mountainous Mediterranean climate North Yuba River, California, watershed and its reservoir near the downstream outlet. Over a 30-year study period, 1985–2014, volumetric estimates of annual wood export into the reservoir, available for a subset of years, were used to investigate watershed-scale wood export dynamics. Variations in annual peak discharge explained 79% of the variance in interannual wood export, with 84% of total observed wood export (ca. > 10,000 m^3 of wood per event) delivered by three discharge events of 19-year, 21.5-year, and 60-year flood recurrence intervals. Continuous video monitoring conducted during snowmelt season periods in 2010 and 2011 yielded wood discharge observations at minima 15% of statistical bankfull flow, while maximum daily discharge explained 55% of observed daily wood piece variation. No statistically significant wood discharge differences were found in snowmelt season observations, likely because of domination of the hydrograph by diurnal pulses within the seasonal cycle. A conceptual model and functional framework are introduced in support of a watershed-scale explanation of wood export, transport, and storage processes applicable to large, Mediterranean-climate, mountain watershed settings.

Keywords: Wood export, Mountain watershed, Large river,

Mediterranean climate

1.0 Introduction

Scientific understanding of wood as a mechanistic agent in riverine environments has expanded since reports from the Pacific Northwest United States detailed adverse effects brought about by forestry extraction practices. Logging to stream edge and clearing wood out of streams alters channel morphology, increases sediment transport, and leads to declines in aquatic productivity (Swanson et al., 1976; Anderson et al., 1978; Bilby and Likens, 1980; Bilby, 1985; Harmon et al., 1986; Bisson et al., 1987). An early and enduring conceptual framework of wood dynamics described important physical and bio- logical drivers and processes that deliver, store, break down, and move wood through stream channels (Keller and Swanson, 1979).

The introduction of a wood budget equation provided a quantitative framework of known first-order constraints on wood dynamics in streams (Benda and Sias, 2003; Benda et al., 2003). Wood budgets use conservation of mass principals to enumerate wood inputs, outputs, and the processes in between in a manner analogous to hydrologic and sediment mass balance budgets (e.g., Curtis et al., 2005; Merz et al., 2006). Construction of complete wood budgets remains infrequent (but see Martin and Benda, 2001; MacVicar and Piégay, 2012; Schenk et al., 2014) because of the breadth of necessary wood data collection elements, which can be summarized into recruitment, storage, decay, transport, and export categories (Benda and Sias, 2003; Swanson, 2003; Hassan et al., 2005), and the complexity of additional mechanisms in the surrounding environment that contribute to the stochastic regulation of these wood variables (Gregory et al., 2003; Wohl et al., 2010; Wohl, 2016).

Efforts to understand, describe, and quantify wood processes have advanced substantially (e.g., Gurnell et al., 2002; Gregory et al., 2003; Wohl et al., 2010; Merten et al., 2010; Ruiz-Villanueva et al., 2016; Wohl, 2016), yet research activities are still emerging in efforts to identify and quantify stochastic complexities between wood processes and hydrologic variations, climatic forcings, and watershed processes. The purpose of this study was to explore how watershed-scale wood processes vary under multiscalar hydrologic regimes and associated climate forcings.

1.1. Wood dynamics

Investigations that have focused on linkages between stream discharge (Q, volume/time), wood discharge (Q_w, volume/time) or wood piece discharge (Q_{wp}, piece count/time), and climate forcings have taken advantage of reservoirs as depositional zones where cumulative wood export quantities (W_{exp}, volume or piece count on an event to multiyear basis) can be surveyed within the context of other water- shed characteristics. A reservoir study in France revealed that large Q peaks delivered large quantities of W_{exp} but antecedent conditions had a dampening effect during subsequent Q peaks (Moulin and Piégay, 2004; Veronique et al., 2016). Across a wide range of reservoirs in Japan, peak annual Q (Seo et al., 2008) and latitudinal variations in precipitation were significant factors in explaining differences in W_{exp} quantities (Seo et al., 2012), with typhoon-generated flooding delivering more W_{exp} into reservoirs even though less stored wood was available for transport in watersheds with higher precipitation totals (Seo et al., 2015).

Technological advances in remote sensing capabilities have opened access to wood dynamics at wider spatial and temporal scales than a field campaign alone can attain (MacVicar et al., 2009). A combination of satellite imagery analyses, reservoir surveys, and channel surveys was effective in assessing total W_{exp} after Typhoon Morakot in Taiwan, where landsliding was the dominant delivery mechanism (West et al., 2011). Video imagery collected from channels and a reservoir shoreline during helicopter flights was used to estimate total W_{exp} after an extreme rain event caused landsliding in tropical Costa Rica (Wohl and Ogden, 2013). Satellite and aerial imagery was effective at capturing temporal variations in wood accumulations in a complex delta in eastern Quebec, Canada (Boivin et al., 2015). A cost- and effort-effective method to estimate Q_w when wood velocity is sufficiently low may include the use of time-lapse photography and probabilistic sampling of images, as demonstrated by a wood study in Canada (Kramer and Wohl, 2014).

Direct methods of monitoring wood in transport have recently been developed and have the potential to reveal processes as they occur. MacVicar et al. (2009) identified the difficulty of obtaining field data to validate theoretical concepts about Q_w as a technical problem primarily limited by available methods. To solve this, they reported on a proof-of-concept, at-a-station, continuous video monitoring technique that successfully collected Q_w footage on the lowland Ain River, France. MacVicar and Piégay (2012) used that empirical data to refine the theoretical relationship, first presented by Benda and Sias (2003), between Q and Q_w, as written here:

$$Q_w = b(Q - Q_{min})\ and\ b = \left[\frac{Q_{wref}}{Q_{ref} - Q_{min}}\right] \qquad (1)$$

where Q_{min} is defined as threshold Q at which wood begins to transport, and Q_{wref} is defined as Q_w at a Q_{ref} of bankfull discharge. Assuming linearity, b is defined as a slope coefficient found via regression. The simplification of b is useful, as individual parameters are difficult to determine when no data yet exist to establish Q_{wref} values. Analyses revealed higher rates of Q_w on rising limbs of flood hydrographs than on falling limbs, which resulted in development of a two-step linear model that reflected the observed clockwise hysteresis behavior (MacVicar and Piégay, 2012).

Use of a stilling basin and bedload traps allowed Turowski et al. (2013) to collect wood data across three orders of magnitude in mass, 1 g to 3 kg (i.e., particulate to large wood sizes), exporting from a small headwater catchment in the Swiss Alps. They developed a power relation between decreasing number of wood pieces and increasing particle mass, reported in the form of:

$$C = kM^{-\alpha} \qquad (2)$$

where C is the relative fraction of wood with a particle mass C, k is a constant, and $-\alpha$ is a scaling exponent independent of Q. The $-\alpha$ scaling exponent mean was 1.84, with a range 1.41–2.26, using 28 samples. Wood data from the Ain River (MacVicar and Piégay, 2012) yielded a similar $-\alpha$ value of 1.8, which may help to independently support the use of a scaling exponent to predict Q_w frequency (Turowski et al., 2013). Data also revealed a power relation across seven orders of Q_w mass (kg/s) and four orders of Q in the form of:

$$Q_w\ (mass) = aQ^b \tag{3}$$

Two large discharge events not used in the Turowski et al. (2013) development of this rating curve aligned with the upper reaches of the regression line, suggesting continued strength of the relation during higher flood flows.

The use of remotely sensed data collection techniques and the recognition of reservoirs as depositional zones in which to enumerate wood export have thus proven quite valuable in advancing scientific understanding of the interactions between wood, hydrologic regimes, and a suite of watershed-scale environmental factors.

1.2. Study objectives

Within the scope of decadal, annual, seasonal, and daily scale hydrologic regimes and by using field and remotely sensed data collected from the North Yuba River watershed in California, USA, specific study objectives were to (i) use imagery analyses and field data collected from New Bullards Bar Reservoir to investigate decadal, interannual, and winter season patterns of W_{exp}; (ii) analyze at-a-station continuous video monitoring data collected during snowmelt season Q periods in two consecutive years to understand seasonal, event-based, and daily patterns of Q_w and Q_{wp}; and (iii) test for geometric similarities and differences in wood metrics collected in different locations within the watershed. These analyses form the basis for the introduction of a conceptual model that illustrates, and a functional framework that details, watershed-scale wood processes applicable to large, Mediterranean climate, mountain river watersheds.

2.0 Study site

2.1. General setting

The North Yuba River watershed is located in the forested Sierra Nevada Mountain Range of northern California, USA. The watershed originates at an elevation of 2139 m at Yuba Pass and contains 1097 km^2 in area and 1074 river-km of channels to the confluence of Deadwood Creek at the upstream extent of New Bullards Bar Reservoir (hereafter, NBB; Fig. 1). The watershed is unregulated until its termination into NBB and is considered an important test basin for climate change scenarios related to precipitation variation and salmonid refugia (YSPI, 2015). The NBB dam face is 193 m tall with a crest elevation of 599 m (39°23′36.18″ N, 121°08′34.78″ W) and reservoir storage capacity of 1.2 km^3.

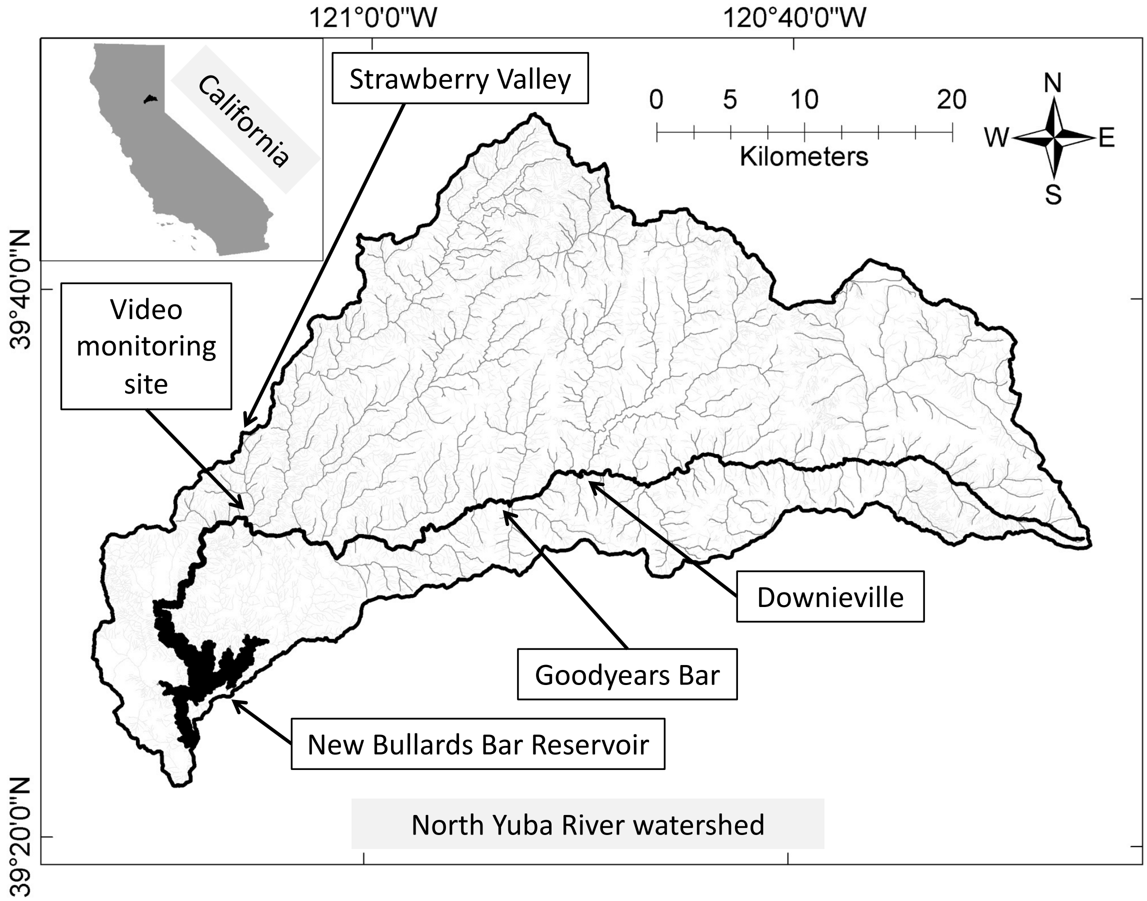

Fig. 1. Geographic setting and field site locations in the North Yuba River watershed, California, USA.

The heavily forested watershed has a disturbance legacy as one of the epicenters of the California gold mining era in the mid- to late 1800s when hydraulic mining operations and other extraction methods dramatically altered stream corridor morphology, riparian continuity, and aquatic ecology (Gilbert, 1917; James, 2005). This economy was supported by intense logging of hillsides that continued to be profitable for decades, so forests are now mostly even-aged stands < 100 years old (Hitchcock et al., 2011). Woody vegetation that enters the channel network and that could transport into NBB includes, in approximate order of increasing elevational bands, foothill California black oak and canyon oak; ponderosa pine, white fir, and Douglas fir in a mixed conifer belt; red fir, Lodgepole pine, and Jeffrey pine; and subalpine tree species including western white pine (Fites-Kaufmann et al., 2007). Riparian corridor species including cottonwood, willow, and alder mix with conifers along larger-order stream banks. Bedrock geology consists of granitic batholith, metamorphosed sedimentary and volcanic rock, and glacial till (Curtis et al., 2005). The channel corridor is largely bedrock-dominated with relatively thin soils 10–100 cm in thickness, inversely proportional to slope (Fites-Kaufmann et al., 2007).

2.2. Hydro-climatic conditions

The climate of the Sierra Nevada is characterized as Mediterranean-montane, with cool, wet winters and warm, dry summers. California's Mediterranean climate experiences yearly drought conditions, with little to no rainfall in the months June through September. Annual precipitation ranges from 500 to 2000 mm depending on elevation and aspect. A rain-snow mix between 500 and 1800 m in elevation is dependent on temperature at the time of precipitation. Approximately 70–90% of precipitation falls as snow above 1800 m from November to March (Mount, 1995). Flood pulses during winter months are often generated by narrow-banded atmospheric river events that can deliver localized, intense, high-magnitude precipitation (Ralph et al., 2006; Dettinger, 2011) nested within low-pressure systems that can deliver moderate to high quantities of precipitation over extended periods of time. The most episodically extreme precipitation events deliver large quantities of warm rainfall onto snow-packed mountain slopes in winter or early spring, initiating rapid snowpack melt that can result in extreme flooding (McCabe et al., 2007; Garvelmann et al., 2015).

Warming springtime climatic conditions drive snowmelt discharge. A progressively warmer diurnal temperature cycle initiates a fluctuating diurnal Q cycle that is a function of daily increases and decreases in snowmelt rates proportional to temperature variations and solar radiation. These fluctuations drive distinct daily Q variations within the larger-scale seasonal rising and recession limbs. The wet winter season is defined for simplicity in this study as October–March, when precipitation runoff exerts the largest influence on hydrographic responses. The snowmelt season is defined as April–July, when snowmelt runoff has the largest influence on hydrographic responses, and the dry season is defined as August–September, when the hydrograph is at a base flow condition. These three seasons constitute one water year (WY, October of a previous year through September of the designation year).

3.0 Material & Methods

3.1. Annual wood export estimation

Each year prior to summertime recreational water activities, NBB management personnel move wood pieces found floating on the reservoir water surface and along the shoreline to one location for safety purposes (Fig. 2). In typical years, wood is burned as a means of disposal when two conditions are met at the beginning of the wet season: enough wood has accumulated to warrant costs and as soon as enough rain has fallen to prevent a fire hazard. If both conditions are not met then the wood is not burned, which can delay disposal for multiple years. In years with episodic flooding and consequently large pulses of W_{exp}, wood is stored in a larger cove and extracted for milling or chipping, depending on piece condition (Fig. 2C). Quantitative data collection of W_{exp} accumulations were obtained from six aerial image analyses (Fig. 3) and three field campaigns (Fig. 4).

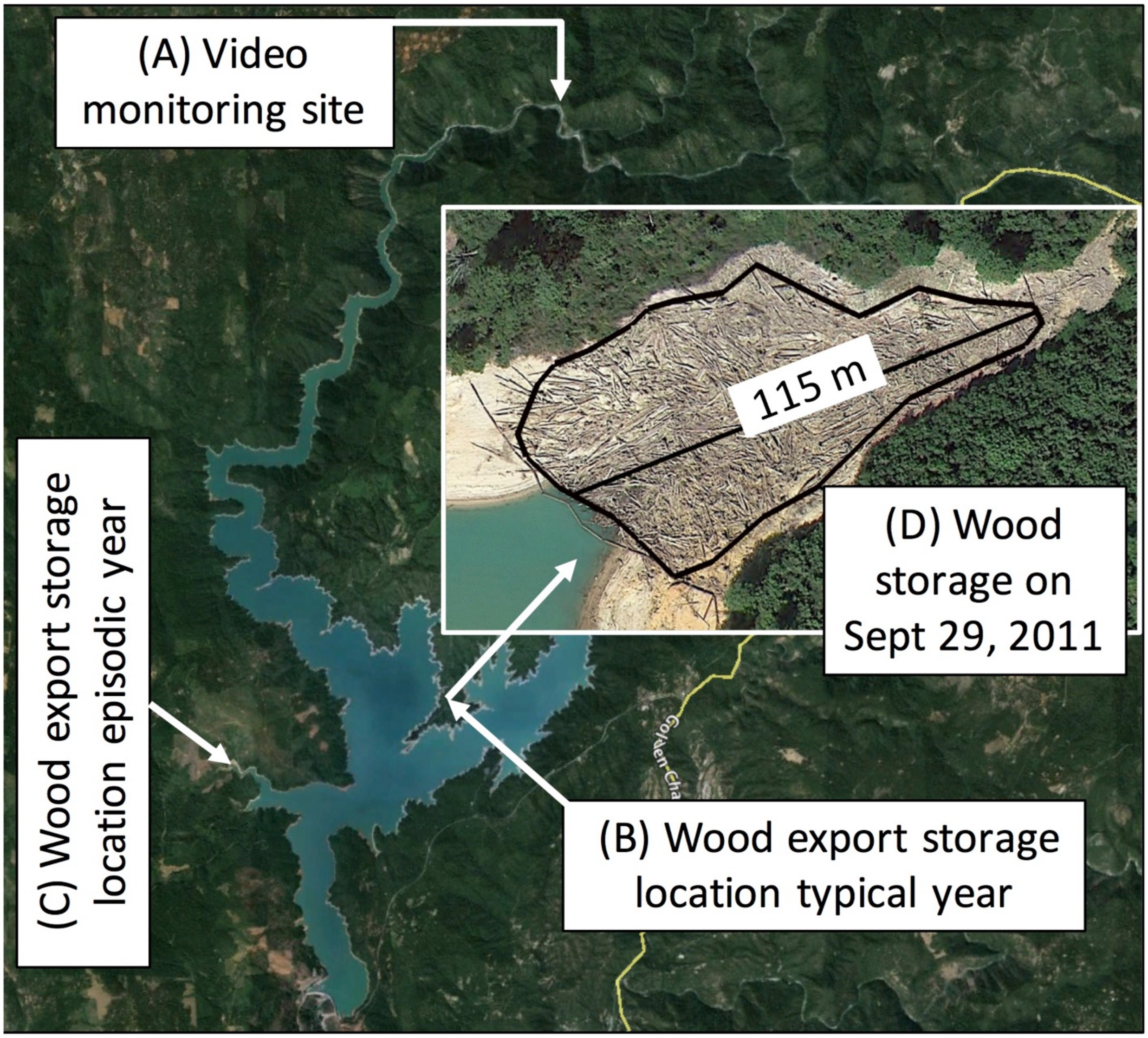

Fig. 2. Google Earth image of New Bullards Bar Reservoir showing (A) video monitoring location at the top of the reservoir, (B) wood storage location in typical wood discharge years, and (C) wood storage location used in years where large floods yield episodically large wood export quantities. Inset (D) shows Google Earth image dated 29 September 2011, which was used to estimate WY2011 wood accumulation quantity.

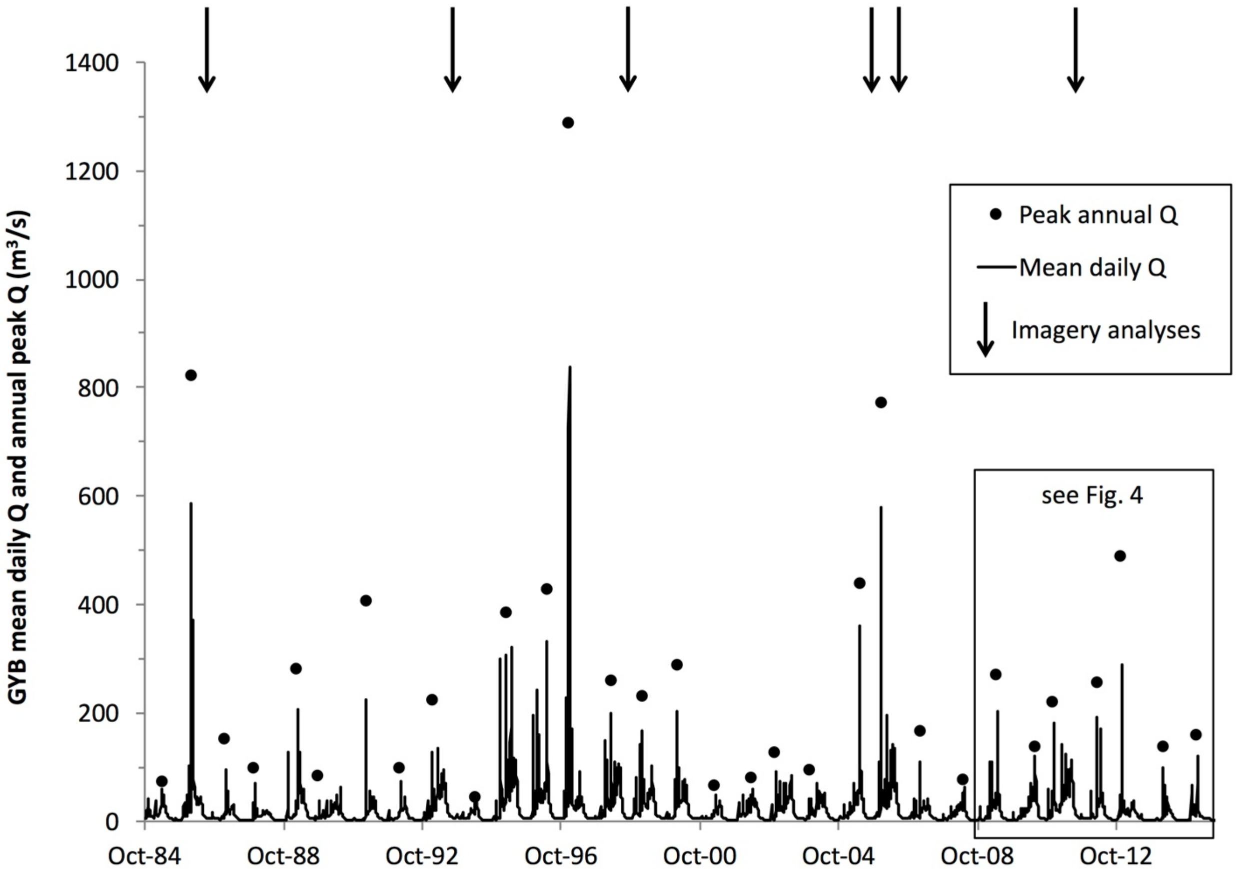

Fig. 3. USGS 11413000 stream gage data, North Yuba River below Goodyears Bar, California. Mean daily discharge and annual peaks for the 30-year period WY1985–WY2014. Arrows indicate dates of aerial imagery analyzed for wood export quantities in Bullards Bar Reservoir. Dots indicate annual peak discharge.

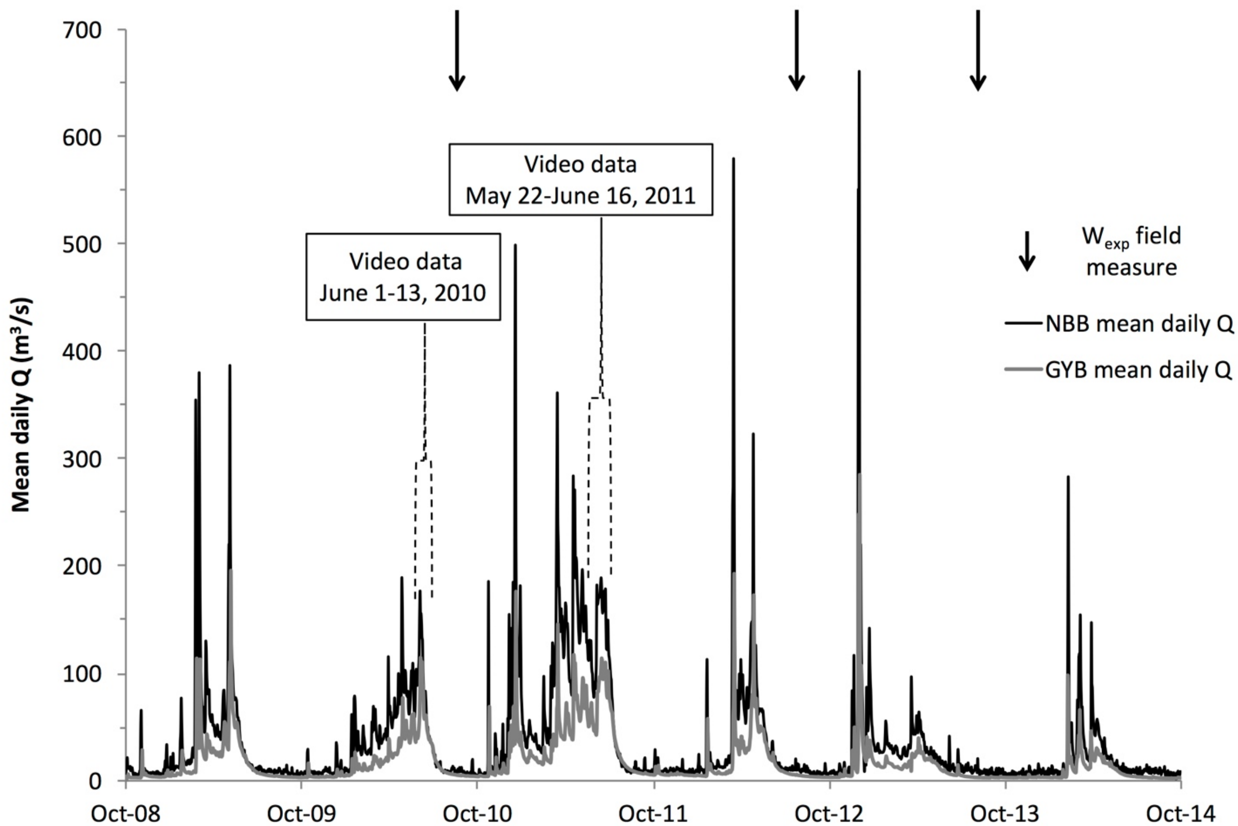

Fig. 4. Mean daily discharge data from Goodyears Bar (gray line) and New Bullards Bar Reservoir (black line), WY2009–WY2014. Video monitoring periods analyzed for wood discharge quantities are indicated by brackets. Arrows indicate dates where field measurements were collected from wood accumulations in New Bullards Bar Reservoir.

Field data collected in WY2010, WY2012, and WY2013 yielded mean wood piece length of 2.8 ± 2.1 m, median 2.0 m, and diameter of 25 ± 18 cm, median 19 cm. Wood density was found by extracting three samples each from 19 wood pieces and performing water displacement analyses that resulted in a wood density estimate of 49 kg/m^3. Each year, a survey starting location was randomly selected along the edge of the accumulation, and then sampling was conducted toward the interior of the pile so that potential porosity variations would be included in the sample (e.g., Fig. 2D). A minimum 100 wood piece lengths and diameters were recorded that met the most commonly used large wood criteria of ≥ 10 cm diameter and ≥ 1 m length (Macka et al., 2011). A GPS unit was used to delineate sampled and total wood accumulation areas. Piece volume was calculated under the assumption that each piece was a cylinder, and then total W_{exp} was calculated (Table 1) using a linear assumption that the sampled area adequately represented the large wood size distribution of the entire accumulation. Although this approach has uncertainties and limitations, the same set of assumptions was used during each field campaign, so measurements contained the same set of biases.

Table 1
Peak annual discharge and total wood export into New Bullards Bar Reservoir.

Water year	NBB annual peak Q	Return interval	NBB W_{exp}	W_{exp} data source
	m^3/s	Years	m^3	
1986	1765	21.5	11925	Landsat
1993	546	2.3	1976	Google Earth
1997	3028	60.0	10800	Landsat
2005	981	7.0	1897	Google Earth
2006	1661	19.0	14125	YWCA[a]
2010	278	0.6	239	field measure[b]
2011	626	3.0	1113	Google Earth
2012	726	4.0	1680	field measure
2013	1132	9.2	83	field measure

[a] Yuba County Water Agency provided image taken from low-flying plane.

[b] $Wexp$ approximated using ratio of yearly peak Q to sum of peak Qs WY2007-WY2010.

Field measurement of 1230 m^3 of wood in WY2010 was associated with four prior years of wood accumulation (Steve Craig, YCWA staff, pers. comm.). Therefore, the wood volume measured in WY2010 was apportioned into WY2007, WY2008, WY2009, and WY2010 using the ratio of each annual peak Q to the sum of annual peak Qs over the four years. This simple calculation yielded estimates for W_{exp} of 110, 421, 469, and 239 m^3, respectively. The estimates were not used in W_{exp} regression analyses but were used as a discussion point about interannual mechanisms. The WY2010 estimate of 239 m^3 was used in comparative analyses with video monitoring Q_w data collected in the same year.

Aerial images obtained from Google Earth (e.g., Fig. 2) were analyzed using online tools embedded in the software to estimate total wood accumulation area. An image from a low-elevation aerial flight in the spring of WY2006 was provided by Yuba County Water Agency, operator of NBB, that documented this particular year's episodically large W_{exp} event (Fig. 5). The image was imported into a GIS and georeferenced to estimate extent of wood coverage. Volumetric estimates (Table 1) for all aerial images were calculated under the assumption that average wood piece sizes and accumulation densities as observed during the three NBB field surveys adequately represented large wood size distributions in all other years.

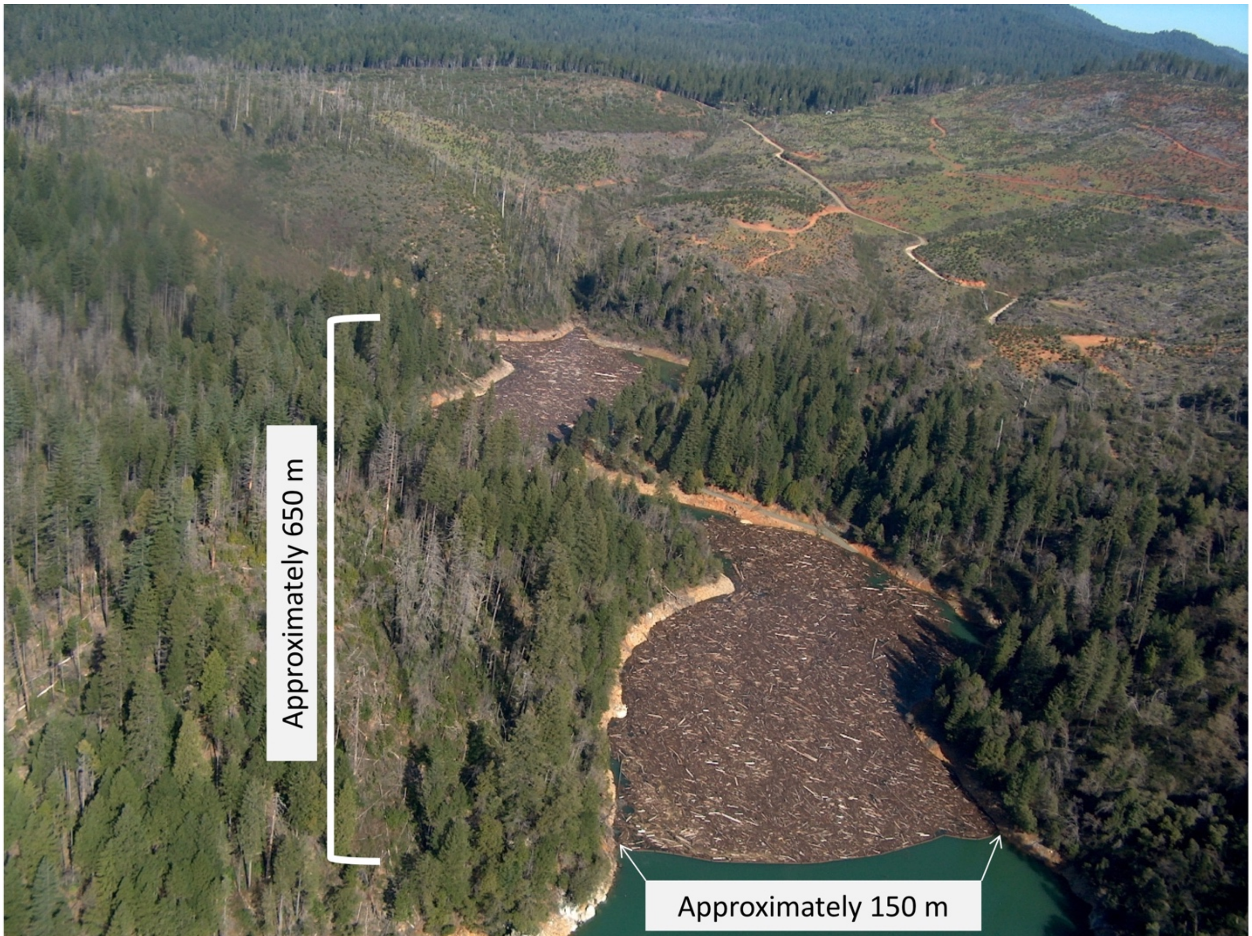

Fig. 5. Aerial image of wood export into New Bullards Bar Reservoir in WY2006 (Fig. 2C location) that was largely as a result of an extreme atmospheric river event in late December–early January. Image taken by Yuba County Water Agency personnel during a reconnaissance flight in April 2006 to assess ongoing wood management activities.

Landsat images with 30-m resolution provided documentation of episodically large W_{exp} events as a result of episodic flooding in WY1986 and WY1997. A comparative analysis was performed to explore uncertainties associated with resolution using a 1-m USGS image taken two days earlier than the Landsat image in 1986 (Gonzalez et al., 2011). The analysis showed that identification errors in the Landsat image could be constrained using a set of spatial coherence tests including dispersion, compactness, and angularity. An identification error rate of ± 15% was found to contain two end members: a 30-m pixel could be falsely identified as containing wood or falsely identified as not containing wood. The method was subsequently used to estimate W_{exp} in a Landsat image from WY1997. Volumetric wood estimates for these two images used the same size distribution assumptions as detailed above. In larger floods, larger wood pieces transport (Merten et al., 2010), so using averaged metrics from more typical years may result in an underestimation of W_{exp} in episodic years. Data from these field campaigns and remotely sensed imagery analyses were used to investigate objective (i), exploration of interannual patterns of W_{exp} into a reservoir.

3.1.1. Hydroclimatic data

Hydrologic data were obtained from the USGS stream gage 11413000 North Yuba River below Goodyears Bar, California (hereafter, GYB Q), elevation 748 m, in the form of annual peak Q and mean daily Q from WY1931 to WY2014, and 15-minute Q data from WY1985 to WY2014. This gaging station collects data from the upper 647 km^2 of the watershed (mean subbasin elevation 1738 m) where the majority of seasonal snowpack accumulates. Downstream tributaries add 450 km^2 of runoff potential into the mainstem from forested mountain slopes between GYB and NBB that are similar in geology, topography, and land cover as the gaged region.

A statistical 2-year (i.e., bankfull discharge) GYB Q return interval of 221 m^3/s was calculated using a Log Pearson type III analysis on the 84-year annual peak Q data set. Hydrologic responses at GYB from the three largest flood events in the 30-year study period occurred in WY1986, WY1997, and WY2006, with recorded peak flows of 821, 1288, and 770 m^3/s, respectively, and flood return intervals of 21, 84, and 14 years, respectively. The hydrograph of the 30-year study period, WY1985–WY2014 is quite variable at annual and seasonal scales (Fig. 3), as is typical of Mediterranean climate hydrology dominated by annual drought conditions. Overlapping GYB Q and NBB Q data show that upstream contributions have a large influence on total hydrographic contributions (Fig. 4), yet downstream contributions can vary in magnitude from those coming from the upper watershed at event and daily scales.

Eight years of annual peak NBB Q data were available (CWR, 2016) but not sufficient for a statistical analysis of peak flow return intervals, so a regression analysis was performed using GYB Q and NBB Q annual peaks from WY2007 to WY2014, which yielded:

$$NBB\ Q_{peak} = 2.04 * GYB_{peak} + 92.43, r^2 = 0.70, p = 0.036 \quad (4)$$

The resulting Eq. (4) was used to construct missing annual peak NBB Q values for the 30-year study period, and then a Log Pearson type III analysis was used to estimate a statistical 2-year bankfull NBB Q return interval of 495 m^3/s. Annual peak NBB Q values for the three largest flood events in WY1986, WY1997, and WY2006 were estimated as 1765, 3028, and 1661 m^3/s, respectively, and return intervals of 21.5, 60, and 19 years, respectively (Table 1).

3.2. Video data collection of seasonal and daily wood export data

An IQeye 750-series power-over-ethernet video surveillance camera and protective casing was installed in June 2010 at the confluence of the remote Deadwood Creek hydropower station, elevation 590 m (39°31′46.51″ N, 121°05′44.92″ W), located at the upstream end of NBB reservoir (Fig. 2A). The powerhouse operates for periods of four to seven months a year depending on enough subwatershed discharge to efficiently generate electricity. Continuous video imagery was successfully recorded during a 2-week period, 1–13 June 2010.

The video camera was reinstalled in January 2011 with the intent of recording Q_w during winter flood peaks. In subsequent winter storms, power lines were disabled twice, requiring site visits to restart the video system. Additional access limitations related to scheduling, weather, and site remoteness resulted in too few days of winter season video imagery to be useful for analyses. Spring weather allowed for easier access and no power failures, leading to successfully collected continuous imagery over the period 22 May to 16 June 2011.

Video image resolution was 2048 × 1536 pixels (3.1 megapixels) with a maximum recording capacity of 16 frames per second. A GBO infinity IL-16-M40-C lens was used to attain focus at all distances within the field of view. When in operation, footage was collected in daylight only. Nighttime recording capabilities were not tested, so the inability to collect 24-hour observations is a study limitation. A near-equinox sun position allowed for visual detection of transporting wood pieces between 06:30 and 21:00 each day. Given observed wood test-piece velocities, imagery recorded at 4 frames per second provided a sufficient number of images for accurate data extraction. The video camera was installed 4.5 m from ground surface (Fig. 6A,B), facing the mainstem perpendicular to flow, on the outside bend of a meander in a bedrock-bounded reach. The field of view contained the lateral extent of the channel (Fig. 6C). Channel width varied with discharge and seasonal timing, averaging about 25-m when NBB was not filled to capacity and flows were unimpeded (Fig. 6D). As NBB filled to capacity, flows at the monitoring site became less turbulent, the gravel bar and eddy zone inundated, and channel width increased to approximately 60-m (Fig. 6C).

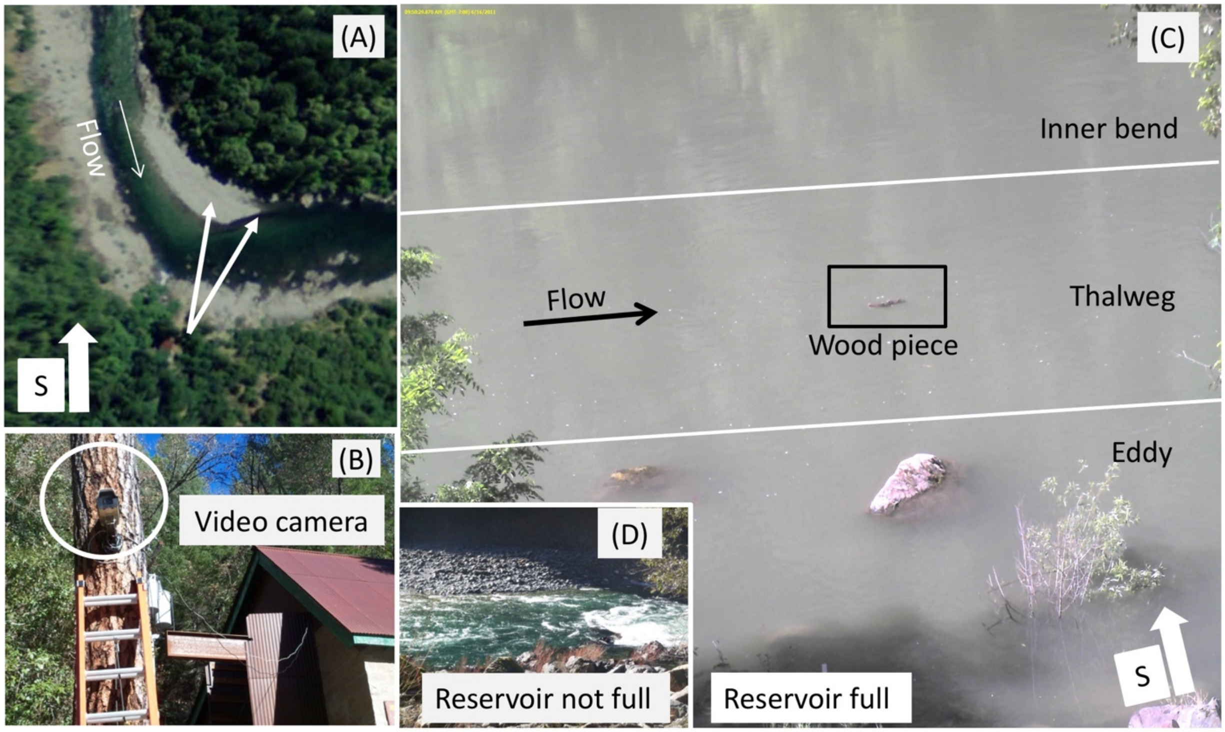

Fig. 6. (A) Video camera monitoring location showing field of view when reservoir is partially full and gravel bar is exposed. (B) Video camera installation adjacent to Deadwood Creek powerhouse. (C) Snapshot of video camera imagery showing identification of one wood piece, lateral zone delineations, and field of view when reservoir is full. (D) Field of view when reservoir is not full.

3.2.1. Wood discharge data extraction

Extraction of wood data from video imagery was performed manually by one analyst and spot-checked by another. Imagery was reviewed using exacqVision video management software from Exacq Technologies, with features that allowed control of the forward and backward speed of 5-minute video clips. Every 5-minute video clip with enough daylight to assess the imagery was viewed in its entirety at least once. Wood pieces were found to be visible for 15–60 s across the field of view depending on discharge, thus, a minimum of 60 individual frames provided adequate opportunity to identify and characterize wood pieces in transport.

To account for distance optics, three zones were demarcated across the lateral extent of the channel (Fig. 6C); wood measures were assumed to remain stable within each zone. An outer bend eddy zone defined the river right bank, the thalweg was visually delineated mid-channel, and the inside bend of the river left bank was defined by an inundated gravel bar during both snowmelt data collection periods. Survey data and eight wood pieces with known dimensions were used to develop conversion factors for distance and angle that were applied uniformly within each zone. Lateral position error in wood length measurements were estimated to be on the order of 5% while lateral position wood diameter errors were likely higher (MacVicar and Piégay, 2012). Both measurements were dependent on a number of factors, including distance from the camera, lighting, buoyancy, and turbulence.

Every wood piece was measured using the pixel-based Jruler v3.1, available online as freeware. Some wood pieces did not formally meet the large wood minimum size criteria of ≥ 10 cm diameter and ≥ 1 m length, but metrics were recorded anyway. An independent repeat-verification process was conducted to assess piece identification and length measurement accuracy. Re-measurement of wood piece lengths resulted in an average and median increase in length of 7 cm and 5 cm, respectively, a measurement error rate of 4%. No error rates were calculated for wood piece diameter at both ends, as those were measured just once. An assessment of identification omission was not conducted, as reviews only included video imagery clips known to contain wood data. However, the verification process found all originally identified pieces plus one additional piece.

3.2.2. Snowmelt season hydrologic data, WY2010 and WY2011

Hourly inflow data from NBB were available from WY2007 to WY2014 (CDWR, 2016), thus providing two hydrologic data sets for the latter portion of the 30-year study period. Hourly observations derived from NBB water surface elevation readings at the dam face were smoothed in a 12-hour moving window because of inherent difficulties in translating reservoir elevations into Q, as evidenced by zero and negative inflow values in the data set. Ratio analyses using WY2010 and WY2011 GYB Q and NBB Q data indicated that a 2:3 ratio generally represented the contribution of upper watershed GYB Q to NBB Q such that a GYB Q of 40 m^3/s was assumed to represent an NBB Q of 60 m^3/s, even though exact proportions were dependent on hydrologic-climatic events and local watershed responses.

From GYB to the top of NBB at Deadwood Creek, the mainstem slope averages 0.75% over a flowline distance of 24.9 river-km. Stream flow lag time was estimated as 9.5 h based on available averaged Q velocities from the GYB stream gage. At NBB, peak day- time temperatures occur mid-afternoon, while peak daily snowmelt Q tends to occur overnight. During the two snowmelt season collection periods, Q_w was observed in both WYs at a NBB mean daily Q of 60–70 m^3/s, which represents about 15% of the statistical bankfull discharge. However, the WY hydrographs were notably different. WY2010 was dominated by low-flow conditions, with just one early spring peak flow larger than the snowmelt season peak flow, resulting in only 16% of NBB Q values > 60 m^3/s over the course of the WY. Conversely, WY2011 had multiple higher magnitude and longer duration Q events in the wet season, resulting in 42% of NBB Q values > 60 m^3/s over the WY. Video footage collected 1–13 June 2010 and 22 May to 16 June 2011 were used to assess objective (ii), analysis of seasonal, event-based, and daily patterns of Q_w and Q_{wp}.

3.3. Network-scale wood storage

Wood storage data from the greater Yuba River watershed (three sub-basins constituting 2874 km^2) were collected in summer of WY2012 (Vaughan, 2013) to gain an understanding of the distribution and volume of wood available for transport within the channel network. Benda and Bigelow (2014) report that recruitment processes in third order Sierra Nevada watersheds are approximately 40% chronic tree mortality and 60% event-based bank erosion, with negligible contributions from landslides.

In Vaughan (2013), a stratified random sampling scheme was used to collect data from 114 reaches 50- or 100-m in length. Measurements were recorded for wood pieces that fit the large wood criteria (Macka et al., 2011) and geomorphic attributes of each wood piece and jam were collected along with morphologic reach characteristics. Total wood volume (wood pieces plus jams) was highly variable between sample sites, yet two metrics, total wood volume per channel length and overbank wood volume per channel length, showed few statistically significant differences between stream orders using Mann-Whitney *U* tests to test for differences greater than zero between mean rank scores of the raw data values at a significance level of $p < 0.05$. In-channel wood distribution, about 14% of total wood volume, exhibited statistically significant systematic decreases in wood volume in the downstream direction.

For this study, 34 reaches located upstream of NBB (Fig. 1) yielded data on 384 individual wood pieces and 110 wood jams. Average active channel width generally increased as stream order increased, ranging from 0.9–39.5 ± 8.9 m with a median of 10.3 m. Almost three-quarters of wood pieces were located along the active channel bank or on the floodplain, with the remainder fairly equally located on bars or in the wetted channel. Wood jams (defined as two or more large wood pieces touching) were mostly associated with bars, with approximately half of jams equally distributed along active channel banks or on the floodplain. About 15% of pieces and jams were located in the wetted channel.

Using Mann-Whitney *U* tests, three of ten wood piece test combinations yielded statistically significant differences. Findings showed that wood piece volume in stream orders 2 and 4 were significantly larger than in stream order 1, and wood piece volume in stream order 2 was significantly larger than in stream order 3. There were no significant differences between wood jam volume by stream order. Jams constituted 75% of total wood volume in the 34 reaches, which led to a broad assumption that wood volume was approximately equally distributed throughout the channel network at a scale of 101 m. These data were used in conjunction with W_{exp} and Q_w size distribution and volume data to assess objective (iii), testing for geometric similarities and differences in wood metrics collected in different locations within the watershed.

3.4. Data analyses

3.4.1. Objective (i)

Investigation of inter-annual variations in volumetric wood quantities used a set of eight W_{exp} values from NBB obtained via field efforts and remotely sensed image analyses. Basic statistics of the data set were explored, including export rates sorted into years with episodically high and more typical annual peak Q values. A wood discharge-rating curve was developed. The resulting equation was used to predict missing W_{exp} quantities over the 30-year study period based on average known conditions, and used in discussing the observed data.

3.4.2. Objective (ii)

Investigation of event-based patterns of Q_w and Q_{wp} during snowmelt season periods in consecutive years was conducted using the two video monitoring data sets. Overlapping Q records were available from GYB and NBB for WY2010 and WY2011 (Fig. 4); both data sets were used in exploratory analyses. Mann-Whitney *U* tests were used to test Q_w length, diameter, and volume associated with Q_w position on the hydrograph against NBB Q magnitudes. Each Q_w and Q_{wp} data set was stratified according to position on the rising or falling limb of a hydrograph defined by two mechanisms: (a) daily, diurnal fluctuations embedded within (b) the seasonal fluctuation. Stratified data were normalized since observation windows and seasonal peak dates differed between years, yielding frequencies that were tested using Chi-square analyses for goodness of fit between observed and expected frequencies at a significance level of $p < 0.05$. Cumulative distributions of length and volume were plotted to explore similarities and differences between years. A frequency analysis was performed following Eq. (2) (Turowski et al., 2013) to test for similarities in $-\alpha$ scaling exponent values. Wood piece lengths and volume for this test were sorted on the basis of the same hydrological mechanisms described above as well as by discharge, and then values were log base-2 transformed, binned by 0.5 increments, plotted, and finally, power functions were calculated via trendline analysis to derive scaling exponent values. The snowmelt transport rate of Q_w as a function of Q was investigated using Eq. (3) (Turowski et al., 2013).

Regression analyses were used to investigate relationships in wood data sorted by individual WY, combined WYs, piece count, length, diameter, and volume. Each data set was regressed against a suite of NBB and GYB Q variables, including mean, maximum, and minimum daily Q and by various Q bins, allowing for exploration of linear functions (Eq. (1); MacVicar and Piégay, 2012). Additional regression analyses excluded days where wood pieces and volume equaled zero, which allowed for exploration of power functions (Eq. (3); Turowski et al., 2013). The most robust outcome was found when Q_{wp} was regressed against maximum daily GYB Q, an analysis that included all non-zero days of data (Table 2).

Table 2

Wood characteristics and stream discharge during continuous video monitoring periods.

Video date	Wood discharge parameters				NBB *Q*	GYB *Q*
	Obs. Wood	Ave. length	Ave. diam.	Est. volume	Daily max	Daily max
	Count	(m)	(cm)	(m^3)	(m^3/s)	(m^3/s)
1-Jun-10	5	2.1	29	0.78	105	68
2-Jun-10	3	1.4	36	0.46	119	81
3-Jun-10	3	2.7	20	0.25	147	107
4-Jun-10	16	1.7	25	1.62	171	131
5-Jun-10	9	2.0	29	1.40	161	134
6-Jun-10	16	2.0	31	2.75	160	137
7-Jun-10	4	1.8	15	0.16	155	130
8-Jun-10	7	1.8	25	0.83	143	107
9-Jun-10	2	1.4	17	0.07	127	98
10-Jun-10	4	2.2	33	0.95	126	94
11-Jun-10	9	1.5	21	0.60	91	65
12-Jun-10	3	1.0	20	0.10	80	67
13-Jun-10	5	1.9	32	0.81	77	67
22-May-11	2	1.3	7	0.011	128	68
23-May-11	2	1.2	3	0.002	134	68
24-May-11	0	0.0	1	0.000	118	75
25-May-11	3	1.2	7	0.018	130	76
26-May-11	0	0.0	0	0.000	111	66
27-May-11	0	0.0	0	0.000	98	60
28-May-11	0	0.0	0	0.000	94	55
29-May-11	1	1.1	6	0.003	85	53
30-May-11	1	1.3	6	0.004	85	48
31-May-11	0	0.0	0	0.000	76	48
1-Jun-11	0	0.0	0	0.000	93	49
2-Jun-11	0	0.0	0	0.000	86	47
3-Jun-11	2	1.0	5	0.005	83	44
4-Jun-11	0	0.0	1	0.000	88	46
5-Jun-11	1	0.9	3	0.001	113	62
6-Jun-11	19	1.8	11	0.543	182	99
7-Jun-11	7	2.6	8	0.123	169	91
8-Jun-11	3	1.4	9	0.029	164	98
9-Jun-11	5	1.3	12	0.076	165	102
10-Jun-11	8	1.3	7	0.055	172	109
11-Jun-11	6	1.8	9	0.305	170	109
12-Jun-11	5	1.5	10	0.099	174	110
13-Jun-11	13	1.8	9	0.480	175	119
14-Jun-11	19	1.9	6	0.162	187	133
15-Jun-11	43	1.7	6	0.288	189	134
16-Jun-11	11	1.4	7	0.065	187	133

The power function resulting from this initial exploration was then used to predict Q_{wp} over the two snowmelt season observation windows and again for the entire WY Q records for WY2010 and WY2011, in both cases using a threshold value of NBB Q_{min} > 60 m^3/s as this was the lowest Q at which Q_{wp} was observed during video monitoring. This test allowed for exploration of how Q_{wp} and Q_w might respond to hydrologic events smaller than the annual peak Q event. Resulting Q_{wp} values were converted to Q_{wp} using observed wood mean and standard deviation values from the appropriate snowmelt season WY, as well as using mean and standard deviation values that represented the full range in wood piece metrics as derived from the combined three sets of W_{exp} field measurements, two sets of Q_w measurements, and one set of upper watershed field measurements; this combined set is reported as global values. Within the two snowmelt observation periods, this analysis provided a test of whether the video monitoring data extraction process was able to identify most wood pieces in transport compared to a predicted value. At the WY-scale, comparisons between Q_{wp}, Q_w, and W_{exp} provided a test of how Q_w video extraction measurements compared to W_{exp} estimates for those two years.

3.4.3. Objective (iii)

Investigation of wood piece length, diameter, and volume characteristics collected by different methods in different locations in the watershed were compared using W_{exp} and Q_w data as well as data from wood storage locations surveyed in the upper watershed. Basic statistics for each data set are reported via box plots for all wood pieces that met the large wood criteria. This standard resulted in inclusion of all wood pieces from each data set, with the exception of Q_w pieces from WY2011, where just 44 of 151 pieces met the large wood criteria. Wood metrics represented in the box plots were tested via Mann-Whitney U tests. Identical letters indicate data sets with no statistically significant differences.

4.0 Results

4.1. Inter-annual wood export into NBB

Eight volumetric estimates of NBB W_{exp} totaled 43,599 m^3 and varied by four orders of magnitude (Table 1) with mean, standard deviation, and median values of 5095 ± 5493 m^3 and 1976 m^3. In the three WYs with episodically large flooding events, WY1986, WY1997, and WY2006, volumetric estimates of episodically large NBB W_{exp} were > 10,000 m^3, yielding wood export rates at the watershed-area scale of 10–12 m^3/km^2 and at the channel network scale of 10–13 m^3/river-km. These rates convert to wood mass export of about 500–600 kg/km^2 and 500–600 kg/river-km. Volumetric estimates of observed NBB W_{exp} in years with more typical annual peak Q events ranged from about 100 to 2000 m^3, yielding wood export rates at the watershed-area and channel network scales of 0.1–1.8 m^3/km^2 and 0.1–1.8 m^3/river-km, respectively. These export rates convert to wood mass export during smaller annual peak Q events in the range of about 5–100 kg/km^2 and 5–100 kg/river-km.

A power equation explained 79% of variance as a function of NBB annual peak Q, using seven of eight observed W_{exp} values. The WY2013 value was considered an outlier and was not used in the analysis (Table 1, Fig. 7).

$$W_{exp} = 0.0797 * NBB\ Q^{1.5372}, r^2 = 0.79, p = 0.02 \quad (5)$$

The power exponent indicates that a doubling of Q would increase W_{exp} by a factor of about 3.0. First-order estimates of missing W_{exp} values across the 30-year study period were calculated by applying Eq. (5) to each NBB annual peak Q estimate, yielding both under- and over-predictions of known values as a function of the variability in the observed data set. Overall, predicted W_{exp} was 68,315 m^3 over the 30-year period with a range of ~ 19,000–30,000 on a decadal basis (Table 3, Fig. 8). All predicted values of known values fell within about ± 50% of observed, except for the previously identified W_{exp} outlier in WY2013 that was greatly overpredicted, and WY2006 that was about two times larger than predicted.

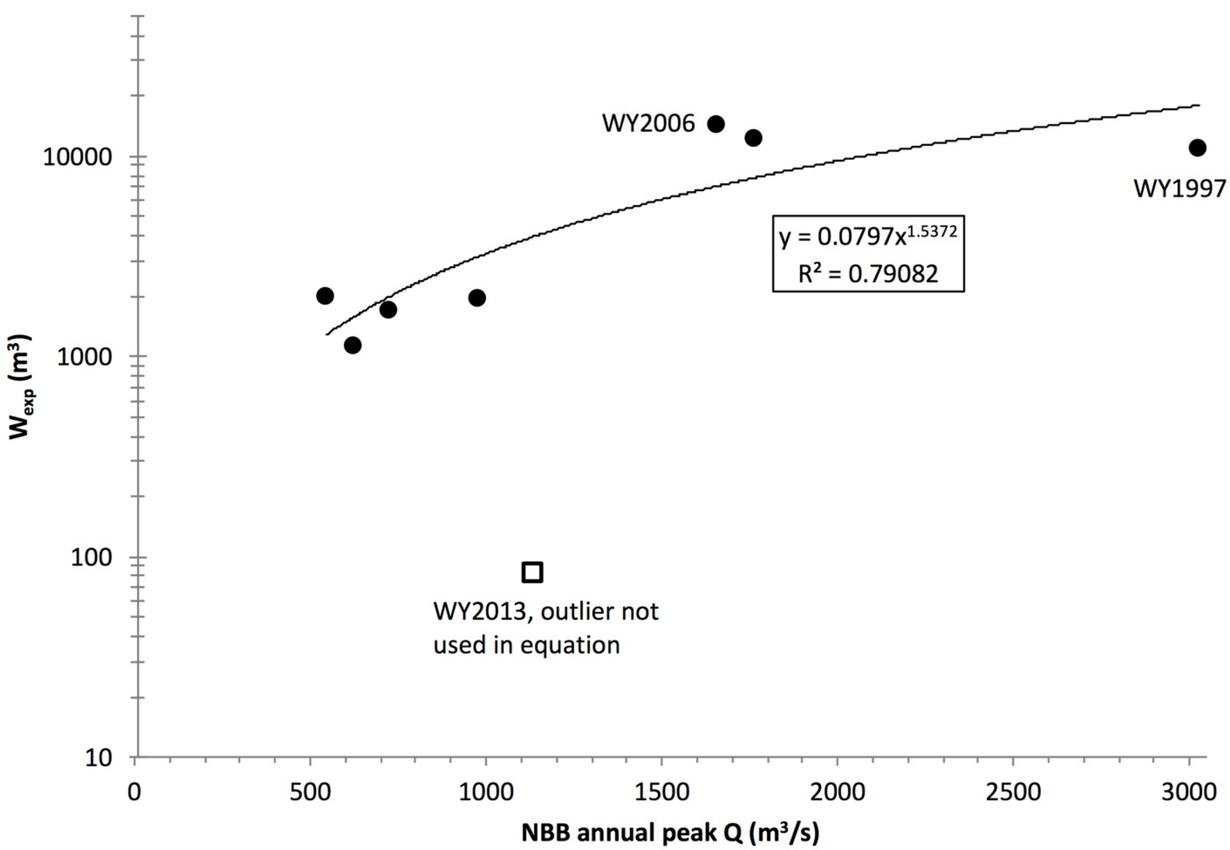

Fig. 7. Wood export rating curve using seven annual volumetric estimates of wood export into New Bullards Bar Reservoir.

Table 3
Comparison of observed and predicted W_{exp} (m^3) into NBB.

Water year	NBB Q peak, m^3/s	Observed W_{exp}	Predicted W_{exp}, Eq. (5)
1986	1765	11,925	7803
1987	403		807
1988	289		484
1989	663		1734
1990	262		416
1991	917		2853
1992	288		481
1993	546	1976	1284
1994	179		231
1995	871		2635
1996	963		3076
1997	3028	10,800	17893
1998	620		1561
1999	561		1341
2000	675		1780
2001	222		321
2002	250		388
2003	350		648
2004	280		460
2005	981	1897	3162
2006	1661	14,125	7109
2007	117		120
2008	490		1088
2009	545		1282
2010	278		455
2011	626	1113	1586
2012	726	1680	1992
2013	1132	83	3943
2014	382		742
2015	346		638

586

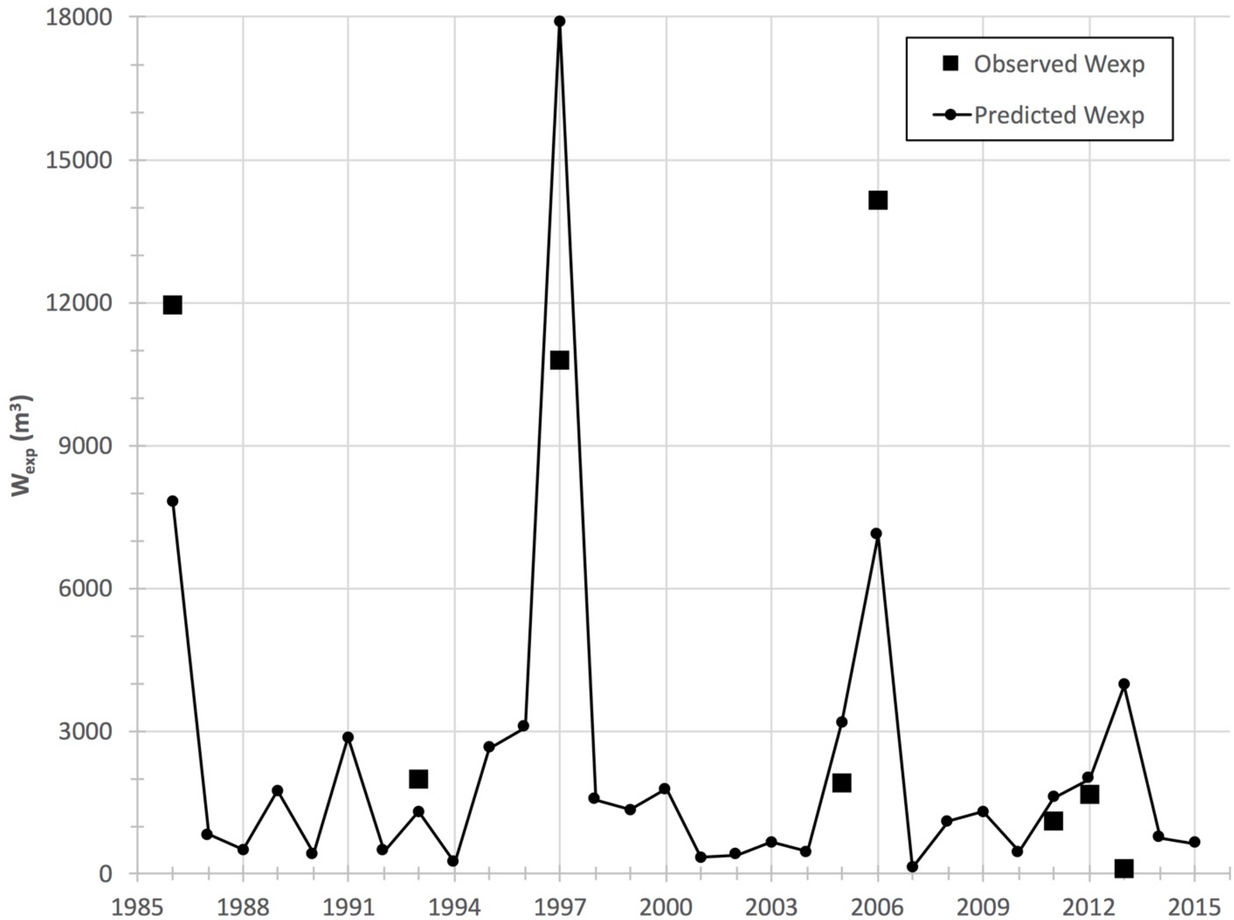

Fig. 8. Observed and predicted wood export volume.

The three largest W_{exp} years with flood return intervals of 19-, 21.5-, and 60-years constituted 36,850 m^3, which represented 84% of total observed W_{exp} and 54% of predicted W_{exp}. On a decadal scale, a ratio analysis between the largest observed W_{exp} in each of the three 10-year periods (e.g., WY1986–WY1995) to the remaining nine years indicated that ~ 50% of total NBB W_{exp} can be attributed to wood activation and transport during statistically infrequent flood events.

4.2. Event-based patterns of Q_w and Q_{wp} during two snowmelt runoff periods

Observed wood discharge in WY2010 equaled 86 pieces for a total of 10.8 m^3 (Table 2) over a period of 180 daylight hours. The average rate of Q_{wp} during this snowmelt period was 0.12 wood pieces per 15-minute increment for a volumetric Q_w rate of 0.015 m^3 per 15-minute increment. The highest Q_w observed in one 15-minute segment was during the 14:00 hour on June 4th when 3 pieces totaled 0.47 m^3, four hours after seasonal peak Q occurred at 10:00 (Fig. 9).

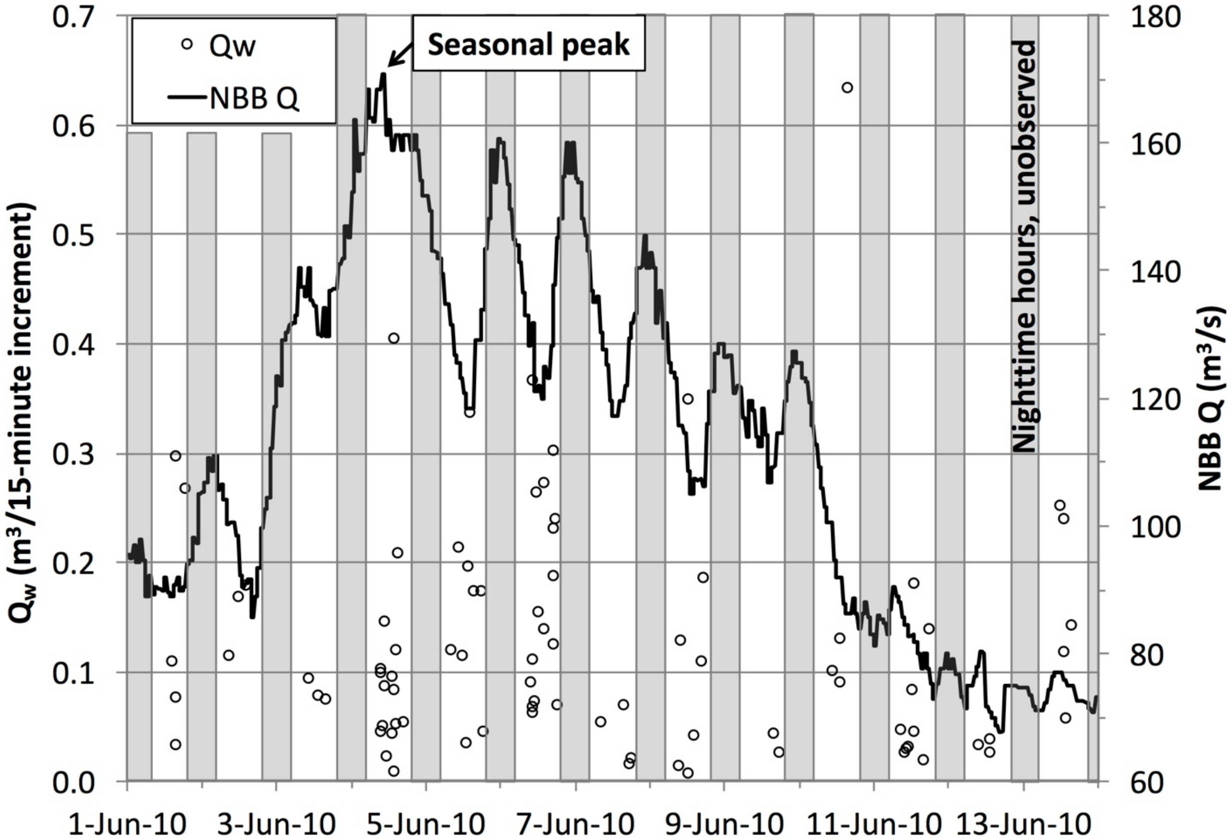

Fig. 9. Partial WY2010 snowmelt season wood discharge and New Bullards Bar Reservoir stream discharge data as a function of time. Shaded areas indicate nighttime hours where wood observations were not possible.

Although the observed wood piece count was higher in WY2011 than in WY2010, total wood piece volume was considerably smaller. Observed wood discharge in WY2011 equaled 151 pieces for a total of 2.3 m^3 over a period of 365 daylight hours. The average rate of Q_{wp} during this snowmelt period was 0.17 wood pieces per 15-minute increment for a volumetric Q_w rate of 0.0025 m^3 per 15-minute increment. The highest Q_w observed in one 15-minute increment was during the 08:00 hour on June 15th when 4 pieces totaled 0.025 m^3, six hours after seasonal peak Q occurred at 02:00 (Fig. 10).

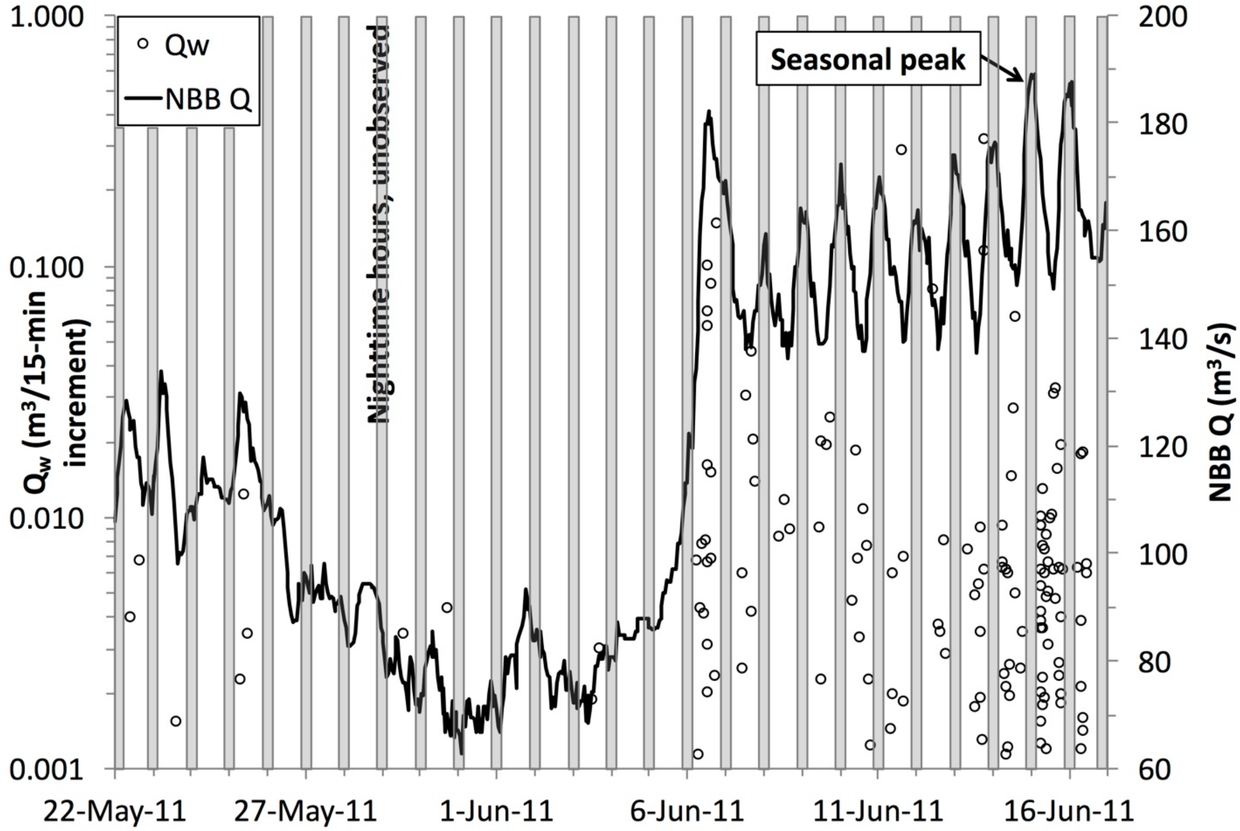

Fig. 10. Partial WY2011 snowmelt season wood discharge and New Bullards Bar Reservoir stream discharge data as a function of time. Shaded areas indicate nighttime hours where wood observations were not possible.

There were no significant differences in either year between wood length, diameter or volume associated with Q_w position on the hydrographs when tested against NBB Q. Normalized wood piece number and wood volume frequencies were statistically indistinguishable from expected when sorted into diurnal rising and falling limbs, and into seasonal rising and falling limbs (Table 4). Cumulative frequency plots show that length measures were approximately equivalent between years, but volumes were not (Fig. 11). Log-binned frequency analyses revealed a wide variety of $-\alpha$ scaling exponent values. Wood piece lengths grouped into WY2010, WY2011, and combined WYs yielded $-\alpha$ exponent values of 2.19, 1.83, and 1.91, respectively. Transport rates of Q_w as a function of discharge were orders of magnitude lower than predicted by Eq. (3).

Table 4

Wood discharge snowmelt season characteristics and χ^2-test results.

	Diurnal		Seasonal	
	Rising	Falling	Rising	Falling
WY2010 Wood piece count	32	54	16	70
Observed frequency, Q_{wp} per 15-minute	0.113	0.115	0.085	0.124
Expected frequency	0.114	0.114	0.114	0.114
Significant difference?		no		no
p -Value		0.95		0.17
WY2010 Wood volume (m^3)	4.0	6.8	8.9	1.9
Observed frequency, Q_w per 15-minute	0.014	0.014	0.010	0.016
Expected frequency	0.014	0.014	0.014	0.014
Significant difference?		no		no
p -Value		0.98		0.58
WY2011 Wood piece count	55	96	97	54
Observed frequency, Q_{wp} per 15-minute	0.096	0.102	0.107	0.089
Expected frequency	0.10	0.10	0.10	0.10
Significant difference?		no		no
p -Value		0.73		0.28
WY2011 Wood volume (m^3)	1.10	1.17	1.17	1.10
Observed frequency, Q_w per 15-minute	0.0019	0.0012	0.0013	0.0018
Expected frequency	0.0015	0.0015	0.0015	0.0015
Significant difference?		no		no
p -Value		0.74		0.80

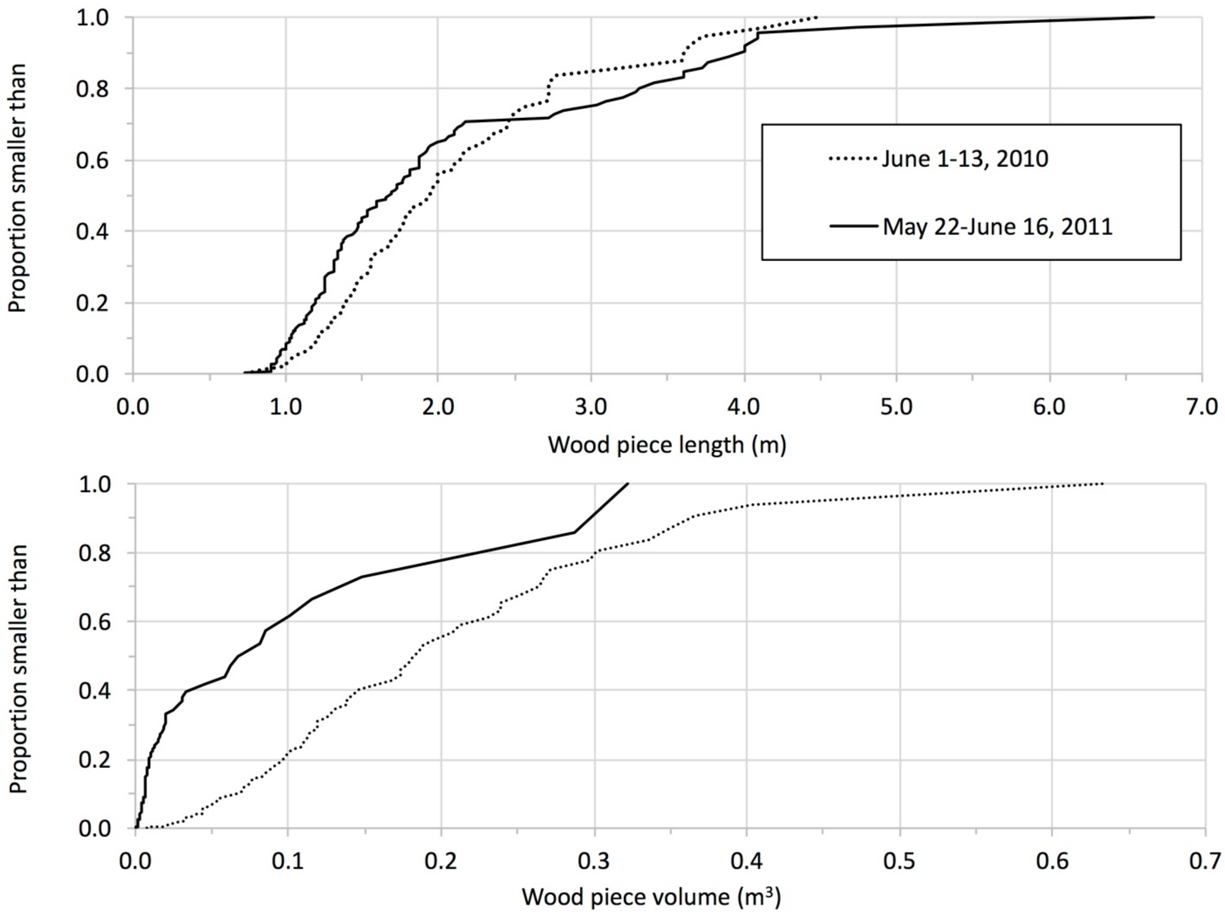

Fig. 11. Cumulative wood length and volume distribution of wood discharge data collected via continuous video monitoring during snowmelt periods in WY2011 and WY2012.

Variability in the distribution of Q_w and Q_{wp} (Table 2) was best explained by a power relation of Q_{wp} per day regressed against maximum daily GYB Q (Fig. 12).

$$Q_{wp} = 0.0004 \times GYB\ Q^{2.113}, r^2 = 0.55, p = .001 \quad (6)$$

The power exponent indicates that a doubling of Q would increase Q_{wp} by about a factor of four, at least within the range of GYB Q during observed snowmelt periods. When NBB Q was used instead of GYB Q, r^2 = 0.42. Individual wood piece volumetric variability yielded no discernable relations within years, however there were marked differences between years (Fig. 13).

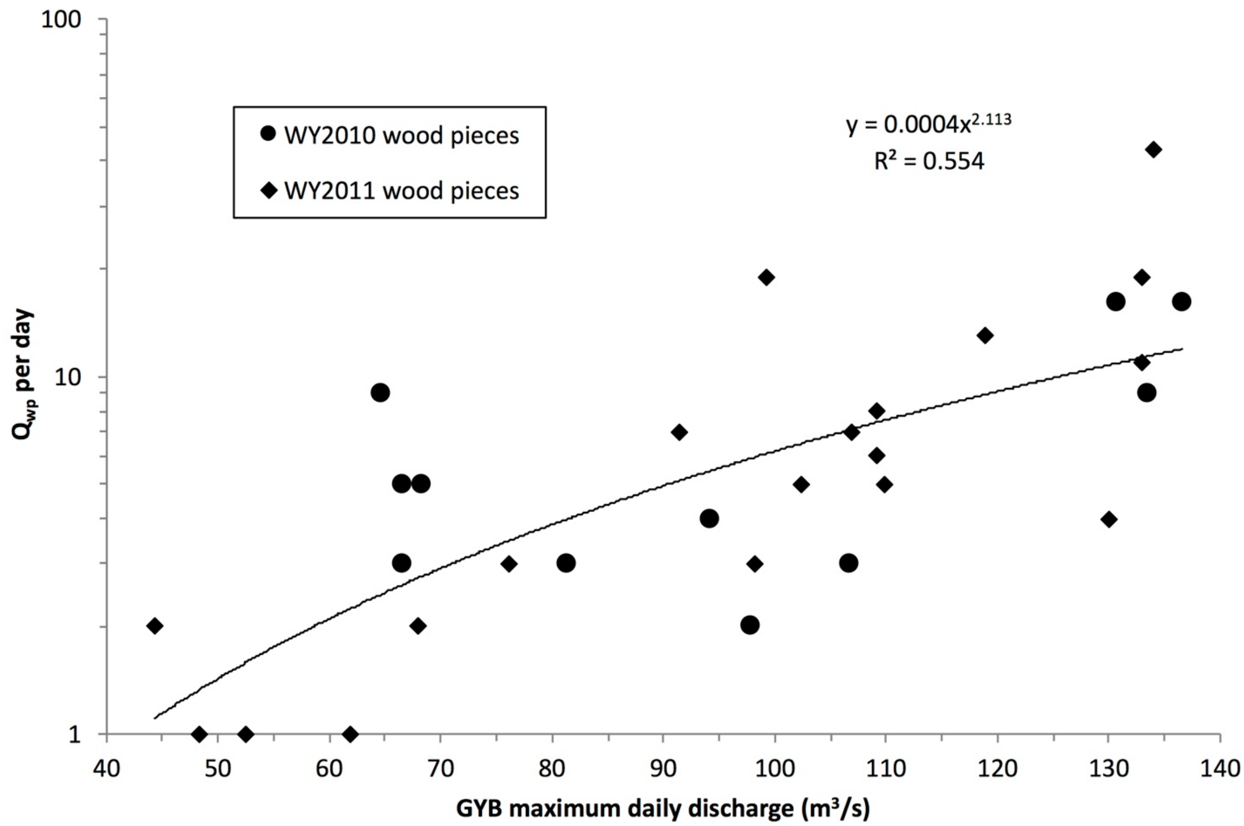

Fig. 12. Observed wood pieces per day regressed against maximum daily stream discharge at GYB provided the best fit in the form of a power function for the combined two years of snowmelt season wood discharge data.

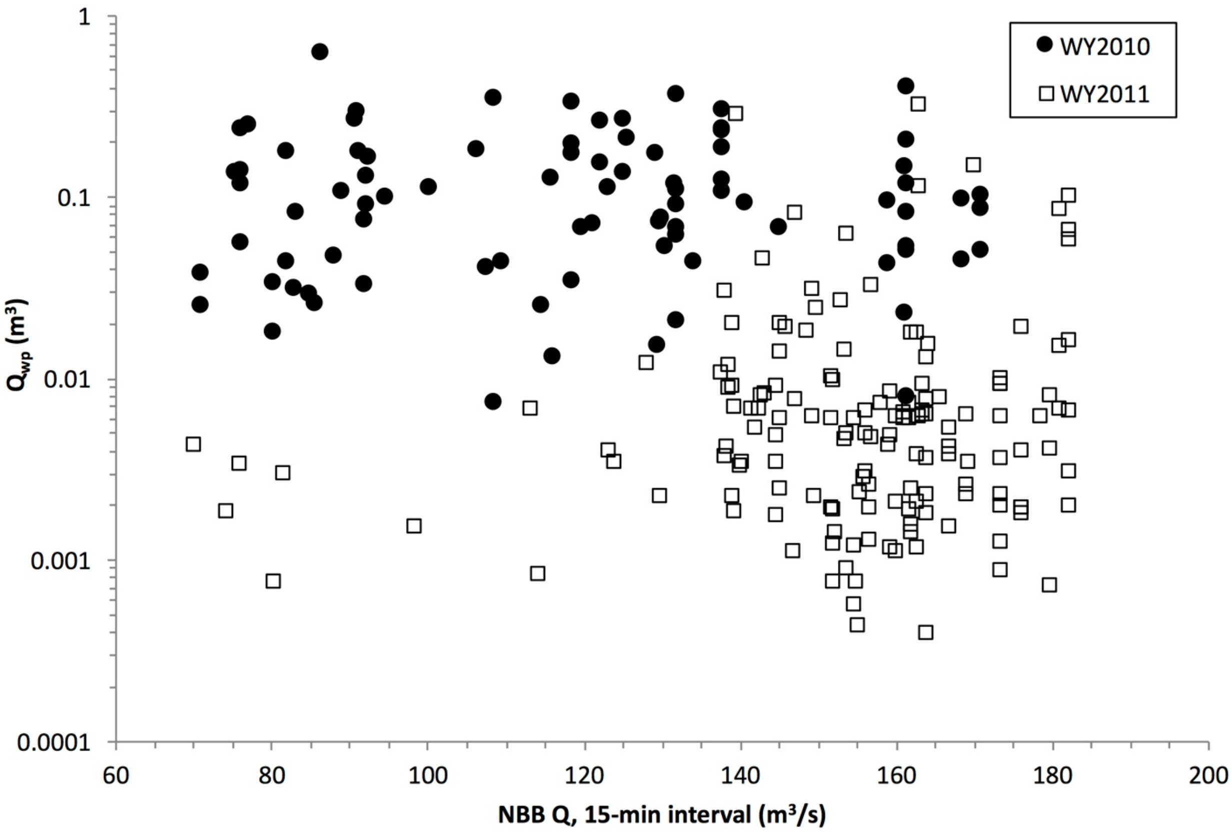

Fig. 13. Variation in individual wood piece volume as a function of New Bullards Bar Reservoir inflow.

When Eq. (6) was applied to all GYB Q > 60 m^3/s within the snowmelt observation windows, Q_{wp} was overestimated in the range of about 30-40% compared to observed (Table 5), suggesting under-identification of wood pieces related to lack of data collection during nighttime hours (Fig. 9, Fig. 10). On the other hand, Eq. 6 yielded underestimates in the range of about 60% compared to NBB W_{exp} piece count estimates, which reinforces the concept of stochastic watershed processes exerting additional controls on wood processes particularly during winter flood conditions.

Table 5

Comparison of observed Q_{wp} and Q_w with Eq. (6) predictions, where NBB Q > 60 m^3/s

	WY2010 June 1-13	WY2010 Total year	WY2011 May 22-June 16	WY2011 Total year
Observed wood piece count, Q_{wp}	86	--	151	--
Observed wood volume, Q_w (m^3)	10.8	--	2.3	--
Estimated NBB wood piece count	--	808	--	4,638
Estimated NBB wood volume (m^3)	--	239	--	1,113
Q_w using NBB wood piece count, and the volumetric parameters:				
Q_w mean[a,b]	--	101	--	70
Q_w standard deviation[a,b]	--	87	--	184
Global mean[c]	--	162	--	927
Global standard deviation[c]	--	443	--	2,539
Q_{wp} result using Eq. (6)	119	320	264	1,976
Q_w using Eq. (6) Q_{wp} result, and the volumetric parameters:				
Q_w mean[a,b]	14.9	40	4.0	70
Q_w standard deviation[a,b]	12.7	34	10.5	23
Global mean[c]	24	64	53	395
Global standard deviation[c]	65	175	145	1,082

[a] WY2010 Qw mean = 0.125 m^3, standard deviation = 0.11 m^3.

[b] WY2011 Qw mean = 0.015 m^3, standard deviation = 0.04 m^3.

[c] Global mean = 0.20 m^3, standard deviation = 0.55 m^3.

4.3. *Wood population variability in the North Yuba River watershed*

Piece length, diameter, and volume of surveyed W_{exp} pieces in NBB were compared to Q_w observed in transport and to wood pieces surveyed in the upper watershed (Fig. 14). Inclusive of all box plot data, wood piece length average and standard deviation was 3.1 ± 3.2 m with a median of 2.1 m, diameter was 23.8 ± 15.1 cm with a median of 19.8 cm, and volume was 0.25 ± 0.80 m^3 with a median of 0.07 m^3.

Wood piece lengths surveyed in the upper North Yuba watershed in WY2012 were significantly different than the video monitoring wood length data sets, but not from the reservoir survey data sets. In the diameter category, upper watershed wood piece diameters were significantly different than all other data sets. Volumetrically, WY2010 Q_w pieces were not significantly different than most other data sets and WY2011 Q_w pieces were significantly different than all other data sets. Other data set associations showed both significant and not significant differences.

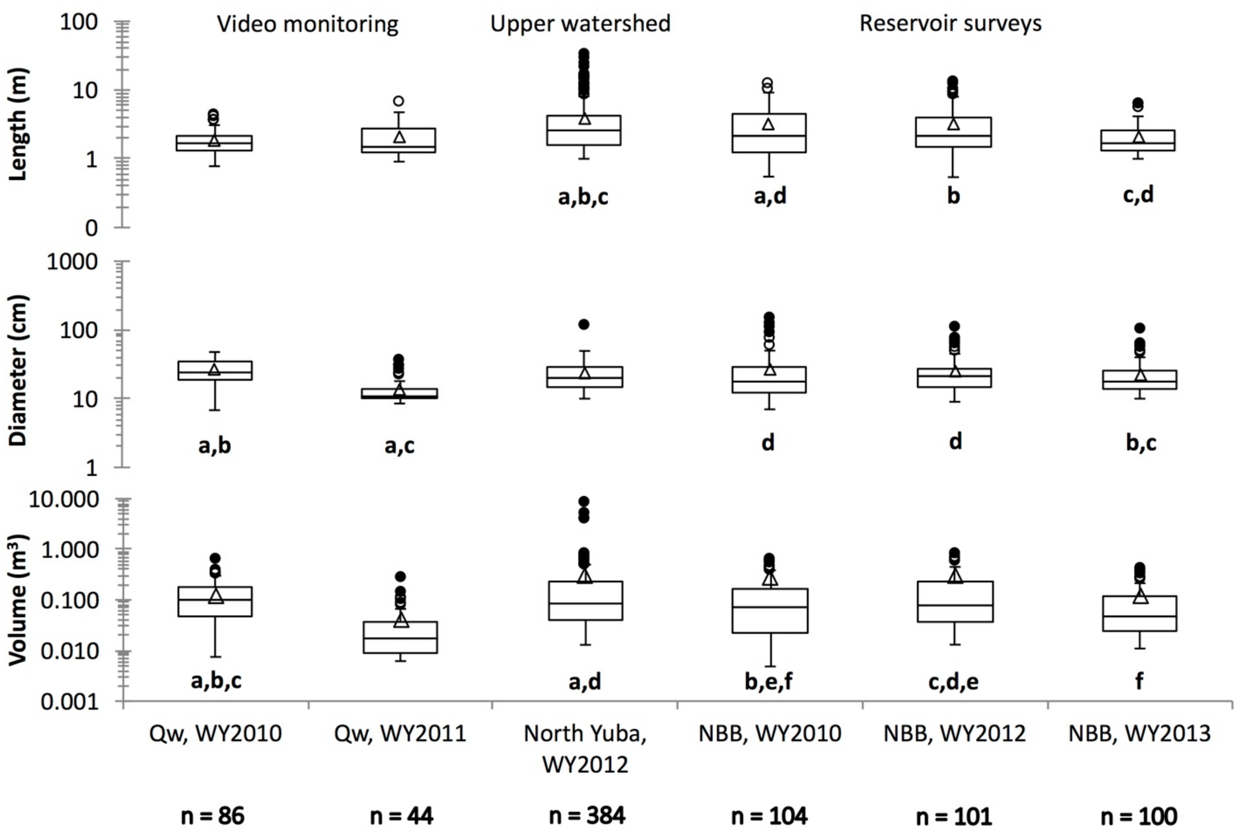

Fig. 14. Summary box plots for length, diameter, and volume metrics from each wood data set. Matched letters indicate Mann-Whitney *U* test results of no significant differences between median ranked values, where $p < 0.05$. Box plot horizontal lines indicate 25th, 50th, and 75th percentiles. The triangle represents the mean. Whiskers represent minimum and maximum values minus the nearest quartile. Open circles and closed circles represent outliers greater than the whisker but less than, and greater than, 1.5 times the interquartile range, respectively.

5.0 Discussion

5.1. Inter-annual mechanisms

Variations in hydrologic conditions associated with annual peak NBB Q explained 79% of the variation found among seven observed W_{exp} values (Fig. 7, Eq. (5)). The explanatory correlation suggests complex interrelationships between variability in decadal and interannual hydrologic responses, the cyclic availability of wood, and a suite of other watershed processes (Moulin and Piégay, 2004; Fremier et al., 2010; Marcus et al., 2011; Benda and Bigelow, 2014). This discussion focuses on how W_{exp} varies in response to hydrologic and climatic variability.

During the three largest wet winter flood event years over the 30-year study period, W_{exp} was climatically driven by atmospheric rivers that delivered intense precipitation via atmospheric rivers (Ralph et al., 2006; Dettinger, 2011) and which initiated episodic W_{exp}

in WY1997 and WY2006. A low pressure meteorological warm rain- on-snow event that triggered rapid snowmelt runoff was the driver of WY1986 peak flows (Kattelmann, 1997), which initiated episodic W_{exp} in WY1986. These three hydrologic events produced 84% of total observed W_{exp} volume (Table 1, Fig. 3) and ~ 50% of total predicted W_{exp} on a decadal scale (Table 3). Recognition of an episodic response in W_{exp} associated with the largest peak flood flows is similar to the observed dominance of episodic Q events associated with large pulses of sediment delivery in Mediterranean climate systems (Gonzalez-Hidalgo et al., 2010).

These observations highlight the linkages between climatic conditions and W_{exp} responses during flood events and identify that two conditions need to be present for episodic W_{exp} responses. First, a hydrologic threshold is necessary to trigger episodic W_{exp} events; and second, enough wood must be available within the watershed to produce episodic W_{exp} volumes (Moulin and Piégay, 2004). In the North Yuba River watershed, the three largest W_{exp} events of the study period recurred on an approximate decadal-scale large-flood return cycle, regardless of Q return interval magnitude. This decadal-scale return cycle is evident in the GYB 30-year flow record (Fig. 3), in the WY1931–WY2014 annual peak flow record, and in historical accounts of California floods (Guinn, 1890; Kattelmann, 1997). The 10 largest annual peak GYB Q values over the 84-year annual peak flow record recurred every 8 ± 5 years, range 2–15 years, with Q ≥ 700 m^3/s in 9 of 10 years. Calculated NBB Q values using Eq. (4) thus provide a first-order estimate of an NBB Q threshold of ≥ 1600 m^3/s (Table 3) to trigger an episodic W_{exp} event of > 10,000 m^3.

Just as in episodic years, years in which smaller quantities of W_{exp} were delivered into NBB may result from a combination of antecedent and current-year hydrologic and climatic conditions. Antecedent flood flows in one WY are known to reduce W_{exp} quantities in subsequent storm events within the same WY (Moulin and Piégay, 2004) and in subsequent WYs following episodic flood events (Marcus et al., 2011). Low W_{exp} quantities in multiple years following episodic W_{exp} events in the North Yuba River may signify flushing of wood from channel margins that require decadal-scale recovery from a wood recruitment perspective. This supposition is supported by examination of the simple annual peak Q ratio analysis of the four-year cumulative WY2010 NBB field measurement, representing WY2007–WY2010. This analysis revealed the relative lack of W_{exp} over the four-year period directly following the episodic event in WY2006, which presumably was related to a temporal lag of new wood recruitment to channel margins (Marcus et al., 2011) and higher than predicted W_{exp} to the watershed outlet in WY2006 (Fig. 8). The anomalously small W_{exp} quantity in WY2013 may be related to the same decadal-scale recovery process or to some other water shed scale factors that remain unknown, such as drought conditions. Future explorations not within the scope of this study might reveal additional hydrologic or watershed mechanisms involved in the anomalously low W_{exp} quantity.

Returning to an examination of the two episodic floods of WY1997 and WY2006, the 60-year flood event in WY1997 delivered 25% less W_{exp} to the watershed outlet at NBB than that 19-year flood event in WY2006 (Table 3, Fig. 8). An explanation may be found by examining the hydrologic record of the two WYs prior to WY1997. Annual peak NBB Q in WY1995 and WY1996 were > 5-year flood return intervals of 871 m^3/s and 963 m^3/s, respectively, in addition to three additional Q events of similar magnitude during those two years (Fig. 3). Application of Eq. (5) resulted in a prediction of W_{exp} > 2500 m^3 for both of those WYs and a W_{exp} prediction for WY1997 of 17,839 m^3 that was much larger than observed. Shortcomings to Eq. (5) will require additional inquiry: the equation relies on annual peak Q only, antecedent conditions are not taken into consideration, and it is not known how long temporal effects last after a previous episodic W_{exp} event, such as in WY1986, which was conversely larger than predicted.

A mechanistic watershed scale explanation is posited here that multiple peak Q events in WY1995 and WY1996 were sufficient to move readily available wood but not sizeable enough to activate widespread bank erosion or to mobilize wood as a result of substantial jam failure—both which are needed for initiation of punctuated large-scale wood recruitment (Jochner et al., 2015) and concurrent episodic W_{exp} transport. Flood events greater than bankfull flows activate available wood within a given water surface elevation into a downstream spiraling pattern (Latterell and Naiman, 2007). Pieces moving through the watershed network deposit into jam or along the channel corridor, disintegrate during transport, or are delivered to the watershed outlet. Chronic wood recruitment potential, meanwhile, continues to supply wood to the channel at approximate baseline rates (Moulin and Piégay, 2004; Marcus et al., 2011).

The subsequent occurrence of a 60-year flood in WY1997 would initiate episodic W_{exp} mechanisms of bank erosion, jam failure, and potentially shallow landslides. However, the ability of chronic wood recruitment to fully resupply the channel margins after two prior years of inferred higher than average W_{exp} is unlikely, and with less readily mobilized wood available for transport, W_{exp} into NBB in WY1997 was substantially reduced compared to predicted (Table 3, Fig. 8).

Episodic mechanisms in WY1997 initiated introduction of numerous new key members for jams (Manners et al., 2007; Jochner et al., 2015) and individual wood pieces into the channel network, potentially with peak wood recruitment delayed until after peak flow. Considering subsequent years (Fig. 3), low peak flows were not large enough to break up jams as a consequence of resistant forces associated with the complexity of rootwads (Braudrick and Grant, 2000). The highest peak flow in WY2005 was associated with diurnal cycle spring snowmelt (Figs. 9,10), so W_{exp} to the watershed outlet would not be expected to be as robust as during a winter storm (Table 6, Fig. 15). The episodic W_{exp} responses in WY1997 and WY2006 varied from predicted as a consequence of complex hydrologic and watershed-scale antecedent mechanisms over annual to decadal scales, indicating that W_{exp} events are not fully independent of previous W_{exp} events or previous flood events. Accordingly, at the annual scale the events of WY1995 and WY1996 played a relatively large antecedent role in the episodic W_{exp} event of WY1997, and at the decadal scale the episodic flood of WY1997 played an antecedent role in the episodic W_{exp} event of WY2006 by delivering additional wood to the channel network that did not fully mobilize until the next episodic flood event.

Table 6

Functional framework for watershed-scale wood responses to seasonality, climatic components, and hydrologic events, in large, Mediterranean climate, mountain river watersheds.

Seasonality	Climatic Component	Hydrologic Event	Wood Response
Summer season, Dry	Light precipitation may occur at high elevations in the form of thunderstorms accompanied by lightening and potential for wildfire. Snowpack gone or negligible.	Base flow hydrograph.	Low wood transport potential, as base flows are not likely to mobilize wood. Wood recruitment potential to resupply wood to channel, banks, and upslope hillsides via tree mortality, limb breakage, tree fall, and dry ravel transporting sediment and wood from hillslopes following wildfire.
Winter season, Dry	Little precipitation with temperatures near or below freezing in upper elevations.	Base flow hydrograph, no elevated flows until watershed moisture regime is seasonally restored.	Low wood transport potential, as lingering base flows are not likely to mobilize wood. Wood recruitment potential same as summer season, dry.
Winter season, Precipitation	Rainfall runoff regime components can result in storm-driven stream flow pulses of varying magnitudes. Snowline is dependent on temperature and will accumulate into snowpack at higher elevations.	Runoff-driven hydrographs. Discharge will increase to above base flow and generally remain elevated through the season, with hydrographic peaks dependent on precipitation patterns.	Wood mobilization and export potential at moderate to high levels depending on hydrologic regime and wood availability. Storm events will mobilize wood, moving pieces downstream. Potential for pieces to deposit against a wood jam or other channel roughness element is high, yet some pieces may export from the watershed. Wood transport distance depends on stream flow magnitude and duration, channel roughness elements, and wood piece resilence. Snow, ice and wind conditions may increase recruitment rates.
Winter season, Atmospheric rivers or stable low pressure systems	Intense or long duration rainfall can result in high cumulative precipitation totals. Snowline is dependent on storm temperature. Snowpack accumulation potential at highest elevations and heavy runoff potential at and below snow line elevations. Episodic storms may deliver warm rain onto snowpack, producing high volume flood flows.	Extreme flood conditions are probable following very intense, high magnitude, or long duration precipitation events. Significant elevated flows may last for up to a week, but peak flood hydrographs generally occur at shorter intervals of one to three days.	Years with episodically large flood events also yield the largest wood export quantities. Water surface elevations initiate wood piece mobility at greater elevational and lateral extents within the channel corridor, floodplains, and adjacent hillslopes. Previously stable jams can break apart from amplified hydraulic forces, increasing the potential for pieces to move long distances with fewer obstacles. Recruitment rates increase with higher rates of bank erosion and limb breakage associated with severe storms. Increased potential of wood additions via hillslope landslides especially in the first year or two after wildfires.
Snowmelt season, Precipitation	Potential for additional snow accumulation with late season precipitation at highest elevations. Or depending on temperature, rainfall may accelerate snowmelt at higher elevations.	Diurnal hydrographs predominate as temperatures and snowmelt fluctuate on a daily basis. Seasonal peak flow is dependent on extent of snowpack, temperature fluctuations, and any additional precipitation. Seasonal falling limb can last up to three months with a large snowpack before returning to base flow conditions.	Wood transport at moderate to low levels depending on magnitude and duration of peak flow and whether most wood pieces available for transport were mobilized and exported or more firmly lodged earlier in the water year. Chronic wood recruitment may provide additional wood supply to the channel.
Snowmelt season, Dry	Little to no precipitation, snowpack is melting and receding, temperatures are warming and eventually no longer fall below freezing.	Diurnal hydrographs predominate with varying peak flows depending on extent of snowpack, daytime temperatures, and temperature fluctuations. Snowmelt season streamflow peaks generally occur in late May or early June, with timing dependent on snowpack and temperatures.	Diurnal peaks may mobilize wood repeatedly to the extent of maximum water surface elevations, moving wood downstream on an incremental, daily basis over a period of days or weeks if a piece does not deposit on channel roughness features that hold it in place. Wood transport/discharge rate may depend on whether wet season floods have already mobilized most pieces that were available for transport. Wood discharge will elevate as snowmelt discharge increases to seasonal peak and then diminish as the snowmelt recession limb progresses toward base flow conditions. In dry water years, snowmelt peak flow can be equivalent to or exceed winter season peak flow. Wood recruitment potential may provide additional wood supply to the channel.

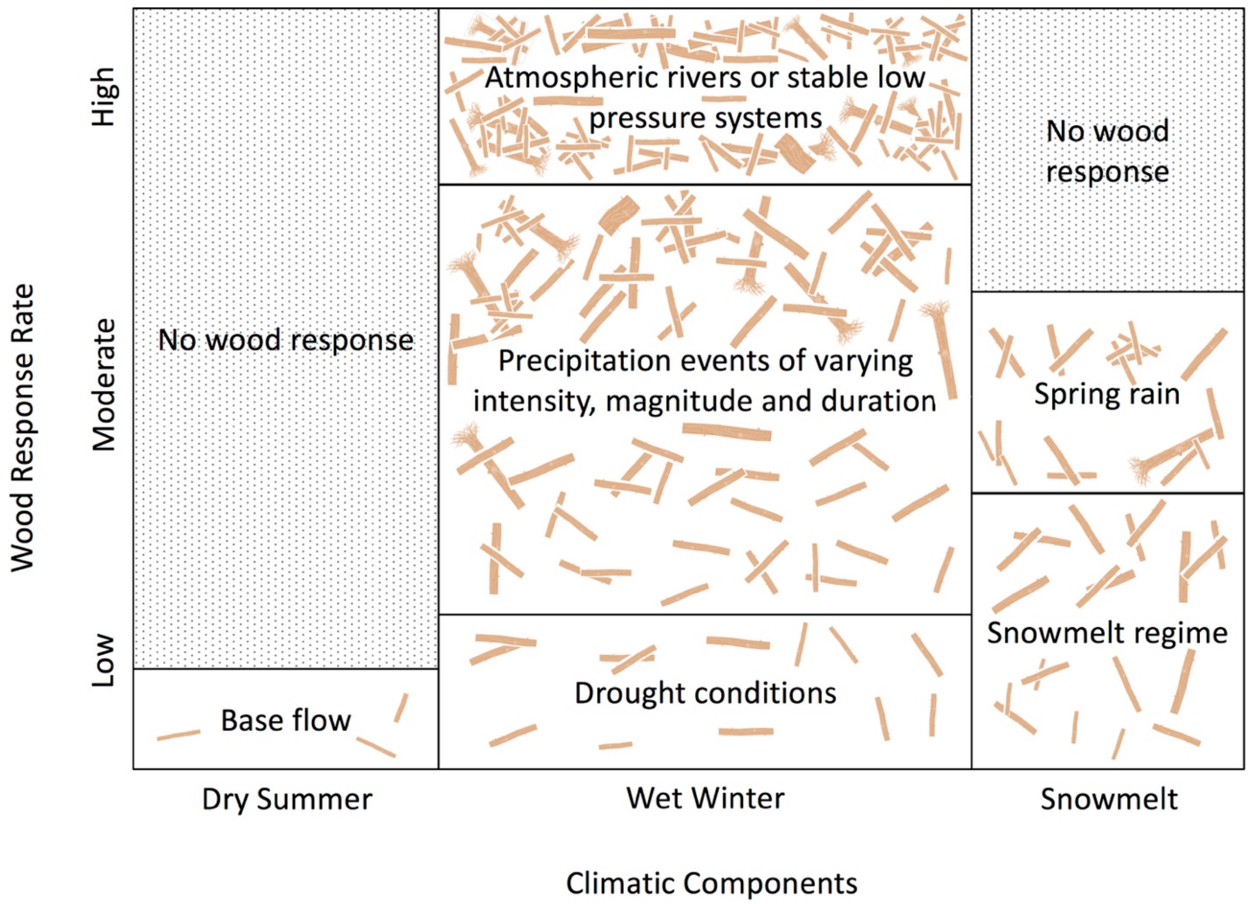

Fig. 15. Conceptual illustration of wood discharge variance as a function of climatological and hydrological dynamics. In dry summer base flow conditions, little to no wood transport occurs, likewise when drought conditions prevail in the winter season. Snowmelt season can generate low to moderate wood response rates, depending on antecedent wood export and winter flow conditions. Winter precipitation events can elicit low to high wood response rates, while spring rains may prompt moderate response rates. Atmospheric river events and other storm systems that deliver unusually intense or large precipitation totals result in high wood response rates.

Wood mass yield per watershed area in the North Yuba River watershed was comparable to average yields of ~ 500 ± 200 kg/km^2 from Japanese watersheds 100–500 km^2 (Seo et al., 2012) during years with episodically large W_{exp}; but in years with more typical peak flows, North Yuba River W_{exp} wood mass yields were much lower than in the Japanese watersheds. Episodically large W_{exp} events are historically important for the delivery of wood to the Yuba River lowlands, while smaller wood fluxes during other hydrological event types are also important for ecological and geomorphic functions throughout the watershed (Keller and Swanson, 1979; Benda and Sias, 2003). Additional work is needed to refine models that predict the degree to which variability in decadal and interannual Q and other watershed processes influence W_{exp} variability.

5.2. *Event-based mechanisms*

A relatively steady supply of individual wood pieces was observed transporting into NBB via continuous video monitoring in the range of 60–190 m^3/s in WY2010 and WY2011 (Figs. 9,10), so 60 m^3/s was considered the lower boundary threshold Q at which Q_w may activate (i.e., Eq. (1), Q_{min}) on the North Yuba River. This Q_{min} constituted about 15% of the statistical bankfull NBB Q, which differs from a Q_{min} of 66% bankfull Q on the Ain River in France (MacVicar et al., 2009; MacVicar and Piégay, 2012), and even more markedly from a Q_{min} of 80% bankfull Q on the Slave River in Canada (Kramer and Wohl, 2014). Similar to having a definition of large wood pieces (Macka et al., 2011) and wood jams (Wohl et al., 2010), a definition of a minimum threshold of wood pieces at which Q_{min} is identified would be beneficial for comparison among studies. In this study, the Q_{min} threshold was defined as one observed wood piece at the lowest observed Q. Differences in Q_{min} between studies may be caused by the duration of observations at a variety of flows in a manner similar to how variations in bedload transport measurements depend on sampling duration and technique (Bunte and Abt, 2005). MacVicar and Piégay (2012) selected relatively short flood hydrograph time frames to analyze, whereas Kramer and Wohl (2014) used sampling techniques to establish Q_w probabilities. Although this study has sampling limitations as well, all video monitoring footage was analyzed.

A simple exercise was used to assess whether a Q-Q_{wp} snowmelt relation (Eq. (6)) could reasonably represent Q_w for the two snowmelt observation periods and across the WYs associated with the video data, using a Q_{min} threshold of 60 m^3/s (Table 5). The differences between volumetric estimates using video monitoring wood piece metrics versus global metrics showed wide variations. Estimated Q_w quantities using the global standard deviation value were most similar to the estimated NBB field measure in both years, an indication that wood piece measurements collected during video monitoring were not fully representative of piece sizes that export into NBB during winter flood conditions. More work is needed to understand how Q_w and Wexp respond to variations in watershed conditions and hydrographic variations, as it seems clear that the small fluctuations in Q during snowmelt season relative to annual peak Q are not a likely mechanism for recruitment of wood pieces in the same manner as flood conditions with respect to bank erosion, jam failure, activation of wood at lateral channel extents, or from gravel bar apices.

Wood responses were relatively similar (Table 2) across the two snowmelt periods in WYs that had very different wet winter storm trajectories (Fig. 4). Notably, Q_w was observed in both snowmelt seasons regardless of antecedent hydrologic conditions earlier in the WY and both minimum and maximum Q were similar even with marked differences in overall WY climatology. The low transport threshold observed in both video monitoring periods may be because of activation of a steady supply of available wood pieces that either reside or fall within the wetted channel margins, and that incrementally spiral downstream during repetitive diurnal rising and falling limbs associated with diurnal temperature fluctuations. Similar wood responses suggest that at the watershed scale, snowmelt mechanisms that drive Q_w are similar across years when the snowmelt hydrograph has similar Q_{min} and Q_{max} values and that antecedent conditions play a smaller role during snowmelt seasons than in wet winter seasons.

Frequency analyses (Table 4) did not indicate hysteresis effects as a function of diurnal or seasonal hydrographs during snowmelt season, which differ from MacVicar and Piégay (2012) observations of a hysteresis effect driven by coupled Q-Q_w behavior during rising and falling limb flood conditions on the Ain River. Additional data in the form of nighttime quantification is needed to continue exploration of diurnal relationships between Q-Q_w on the North Yuba River. However, hysteresis effects may not be present during fluctuating snowmelt Q, as hydraulics and the lateral extents of flows that are less than bankfull are small relative to most WY annual peak Q flood flows, leaving wood transport potential limited to pieces within the wetted channel short enough or thin enough to mobilize.

Wood length frequencies as a function of log-2 scale binning were progressively smaller as length increased, which resulted in scaling exponent $-\alpha$ values in the expected range of 1.8 ± 0.4 (Turowski et al., 2013). Additional relations within the expected range were not found when frequency of piece lengths and volumes were binned by Q or position on the hydrograph. Likewise, predicted wood mass flux using Eq. (3) did not fall within expected ranges. These results may be a function of sample size limitations in two dimensions. Turowski et al. (2013) collected all wood piece sizes, including particulates, while Q maximum was 10^0 m^3/s. Conversely, in this study piece sizes smaller than the large wood criteria were generally not measured and the Q range was 10^1–10^2 m^3/s. To thoroughly test Turowski et al. (2013) methodologies, detailed surveys of all size classes in future NBB W_{exp} accumulations or video monitoring observations over a wider range of Q events would be needed.

This portion of the study verified that the use of video monitoring is practicable in a large mountain watershed setting. Although time-consuming, video imagery can be processed manually, and such an undertaking can now be facilitated by crowdsourcing internet market places for human intelligence tasks. A more reliable power source would be needed to successfully record winter Q_w observations with the system and location used in this study. The lack of winter observations restricts analysis of how Q_w responds to hydrologic variations across a WY, so analyses such as Table 5 require refinement. Direct observations of wet winter flood conditions were not obtained, but Q_w observations coupled with analysis of decadal and interannual W_{exp} were used to provide insight into seasonality associated with Q variations in this watershed.

5.3. Wood population

Multiple significant differences were found in the wood metrics data sets, yet overlap along a common continuum generally supports the presumption that all wood pieces were within the same population (Fig. 14). Insignificant length differences between the upper North Yuba WY2012 data set and most others does not support observations that wood in transport tends to fragment into shorter lengthwise pieces (MacVicar et al., 2009; Schenk et al., 2014), which could be a function of shorter transport distances or wood species piece resilience. Wood pieces in transport may be smoothed but not lose diameter, which may explain why upper watershed diameters were not significantly different from other data sets. Notably, 10% of wood pieces in the upper watershed and an average of 13% of wood pieces across the three NBB field surveys had distinct rootwads in various conditions from fresh to very worn. This similarity in rate of rootwad occurrence suggests that bank erosion processes may be approximately equivalent throughout the watershed such that trees erode from banks into the channel throughout the watershed network and that a small but persistent percentage of wood pieces are fairly resilient to disintegration during transport. At the Q conditions observed during snowmelt, flow hydraulics are not strong enough to transport longer wood pieces (Merten et al., 2010), whereas larger wood pieces are more likely to be transported during higher flows and peak Q events.

5.4. Conceptual model

The acquisition and analysis of spatially and temporally diverse wood data sets and the availability of two hydrologic time series were essential in assembling conceptual and functional first-order linkages between climate, seasonality, hydrology, and wood processes in the large, mountainous, North Yuba River watershed (Table 6, Fig. 15). Eight years of W_{exp} quantities coupled with the 30-year GYB hydrologic data set were key in efforts to conceptualize and describe wood responses to wet winter conditions. Video monitoring data collected over two time periods within consecutive snowmelt seasons coupled with the NBB hydrologic data set helped to conceptualize and describe wood responses to snowmelt conditions. The hydro-climatic drought condition in the Sierra Nevada that brings Q to base flow during dry summer conditions allowed for the presumption that wood transport was essentially zero relative to other seasonal responses. The conceptual model emphasizes how variability in Q can affect variability in wood response as a function of seasonal climatic and hydrologic conditions (Fig. 15). The functional framework synthesizes the complexity of climatological variations, hydrologic responses, and watershed processes that drive wood recruitment, storage, transport, and export (Table 6) according to seasonality, and these complexities are also relevant at multiple temporal scales. The conceptual model and functional framework presented and supported herein may be applicable to other large, mountainous watersheds in Mediterranean climate regions.

6.0 Conclusion

Episodically extreme climatic events and subsequent hydrologic responses were responsible for a large percentage of total W_{exp} on a decadal scale as a function of punctuated hydroclimatic events. Antecedent conditions may exert dynamic and complex effects on W_{exp} rates at decadal, annual, seasonal, and daily scales. Continuous video monitoring was shown to be a practicable method to collect and analyze Q_w as a function of Q, even though processing the imagery was time-intensive. Wood dynamics during snowmelt diurnal cycles embedded within spring snowmelt hydrology do not exhibit hysteresis behavior, as fluctuating Q remained within a narrow range unlike typical flood peaks. Synthesis of data in this study provided the foundation for a first-order conceptual model and functional framework that link seasonality, climate indicators, hydrologic events, and wood response potential at a watershed scale.

The ability to predict W_{exp} may provide planning information to NBB reservoir managers and potentially to other watersheds where similar climatic, discharge, and snowpack mechanisms exist. High-resolution, remotely sensed imagery at yearly to subyearly time steps is now commonly available from Google Earth and other re-sources, so barriers to annual W_{exp} monitoring are rapidly declining. Additional research is needed to explore W_{exp} and Q_w relationships as a function of antecedent conditions, Q return intervals, and multiple smaller peak Q events. Coupling wood discharge monitoring stations with select USGS stream and sediment discharge gaging stations could rapidly increase the quantity of Q_w data and augment opportunities to perform increasingly sophisticated wood dynamics studies.

Acknowledgements

The authors would like to thank Bobby Gonzalez, Denise Tu, Josh Wyrick, and Michael Catania for assistance in the field. Yuba County Water Agency personnel, especially Steve Craig, were helpful in discussions related to reservoir operations and management of wood entering NBB, in allowing access to the field sites, and in providing a secure location for video camera installation. This research was partially funded by an NSF DDIG award [#1031850], two UC Davis Hydrologic Sciences Graduate Group Fellowships, the USDA National Institute of Food and Agriculture [Hatch project number #CA-D-LAW-7034-H], and a Cooperative Ecosystem Studies Unit grant from the U.S. Army Corps of Engineers to coauthor Greg Pasternack [award W912HZ-11-2-0038]. The manuscript was improved thanks to reviews and suggestions from Ellen Wohl, two anonymous reviewers, and the Journal Editor.

References

Anderson, N.H., Sedell, J.R., Roberts, L.M., Triska, F.J., 1978. The role of aquatic invertebrates in processing of wood debris in coniferous forest streams. Am. Midl. Nat. 100 (1), 64–82.

Benda, L., Bigelow, P., 2014. On the patterns and processes of wood in northern California streams. Geomorphology 209, 79–97. http://dx.doi.org/10.1016/j.geomorph.2013.11.028.

Benda, L.E., Sias, J., 2003. A quantitative framework for evaluating the mass balance of in-stream organic debris. For. Ecol. Manag. 172, 1–16.

Benda, L.E., Sias, J., Martin, D., Bilby, R., Veldhuisen, C., Dunne, T., 2003. Wood recruitment processes and wood budgeting. In: Gregory S.V, Boyer K.L. and Gurnell A.M., (Eds.), The Ecology and Management of Wood in World Rivers. American Fisheries Society Symposium, 37. Bethesda, Maryland, pp. 49–73.

Bilby, R.E., 1985. Removal of wood debris may affect stream channel stability. J. For. 82, 609–613.

Bilby, R.E., Likens, G.E., 1980. Importance of organic debris in the structure and function of stream ecosystems. Ecology 61, 1107–1113.

Bisson, P.A., Bilby, R.E., Bryant, M.D., Dolloff, C.A., Grette, G.B., House, R.A., Murphy, M.L., Koski, K.V., Sedell, J.R., 1987. Large woody debris in forested streams in the Pacific Northwest: past, present and future. In: Salo, E.O., Cundy, T.W. (Eds.), Streamside Management: Forestry and Fishery Interactions. University of Washington Institute of Forest Resources Symposium, 57, pp. 143–190.

Boivin, M., Buffin-Belanger, T., Piégay, H., 2015. The raft of the Saint-Jean River, Gaspe (Quebec, Canada): a dynamic feature trapping most of the wood transported from the catchment. Geomorphology 231, 270–280. http://dx.doi.org/10.1016/j. geomorph.2014.12.015.

Braudrick, C.A., Grant, G.E., 2000. When do logs move in rivers? Water Resour. Res. 36 (2), 571–583.

Bunte, K., Abt, S.R., 2005. Effect of sampling time on measured gravel bed load transport rates in a coarse-bedded stream. Water Resour. Res. 41, W11405. http://dx.doi. org/10.1029/2004WR003880.

California Department of Water Resources (CDWR), 2016. Hourly hydrographic inflow data, station BUL. Accessed at http://cdec.water.ca (on March 21, 2016).

Curtis, J.A., Flint, L.E., Alpers, C.N., Yarnell, S.M., 2005. Conceptual model of sediment processes in the upper Yuba River watershed, Sierra Nevada, CA. Geomorphology 68 (3–4), 149–166. http://dx.doi.org/10.1016/j.geomorph.2004.11.019.

Dettinger, M., 2011. Climate change, atmospheric rivers, and floods in California-a multimodel analysis of storm frequency and magnitude changes. J. Am. Water Re- sour. Assoc. 47 (3), 514–523. http://dx.doi.org/10.1111/j.1752-1688.2011.00546.x.

Fites-Kaufmann, J.A., Rundel, P., Stephenson, N., Weixelman, D.A., 2007. Montane and subalpine vegetation of the Sierra Nevada and Cascade Ranges. In: Barbour, M.G., Keeler-Wolf, T., Schoenherr, A.A. (Eds.), Terrestrial Vegetation of California, 3rd ed. University of California Press, Berkeley.

Fremier, A.K., Seo, J.I., Nakamura, F., 2010. Watershed controls on the export of large wood from stream corridors. Geomorphology 117, 33–43. http://dx.doi.org/10.1016/j.geomorph.2009.11.003.

Garvelmann, J., Pohl, S., Weiler, M., 2015. Spatio-temporal controls of snowmelt and runoff generation during rain-on-snow events in a mid-latitude mountain catchment. Hydrol. Process. http://dx.doi.org/10.1002/hyp.10460.

Gilbert, G.K., 1917. Hydraulic-Mining Debris in the Sierra Nevada: U.S. Geological Survey Professional Paper 105.

Gonzalez, R.L., Senter, A.E., Pasternack, G.B., Ustin, S.L., 2011. Measuring stream-wood accumulations in a reservoir using Landsat imagery. Am. Geophys. Union Fall Meet. H13D–1243.

Gonzalez-Hidalgo, J.C., Batalla, R.J., Cerda, A., de Luis, M., 2010. Contribution of the largest events to suspended sediment transport across the USA. Land Degrad. Dev. 21 (2), 83–91.

Gregory, S.V., Boyer, K.L., Gurnell, A.M. (Eds.), 2003. The Ecology and Management of Wood in World Rivers. American Fisheries Society, Symposium. vol. 37. Bethesda, Maryland.

Guinn, J.M., 1890. Exceptional years: a history of California floods and drought. Hist. Soc. South. Calif. 5 (1), 33–39.

Gurnell, A.M., Piégay, H., Swanson, F.J., Gregory, S.V., 2002. Large wood and fluvial processes. Freshw. Biol. 47 (4), 601–619. http://dx.doi.org/10.1046/j.1365-2427.2002.00916.x.

Harmon, M.E., Franklin, J.F., Swanson, F.J., Sollins, P., Gregory, S.V., Lattin, J.D., Anderson, N.H., Cline, S.P., Aumen, N.G., Sedell, J.R., Lienkaemper, G.W., Cromack Jr., K., Cummings, K.W., 1986. Ecology of coarse woody debris in temper- ate ecosystems. Adv. Ecol. Res. 15, 133–302.

Hassan, M.A., Hogan, D.L., Bird, S.A., May, C.L., Gomi, T., Campbell, D., 2005. Spatial and temporal dynamics of wood in headwater stream of the Pacific Northwest. J. Am. Water Resour. Assoc. 41 (4), 899–919.

Hitchcock, E., Rainey, J., Cunningham, F., 2011. A 21st century assessment of the Yuba River watershed. In: A Report by the South Yuba River Citizens League, 2nd ed., (www.yubashed.org, 52 pp.).

James, L.A., 2005. Sediment from hydraulic mining detained by Englebright and small dams in the Yuba basin. Geomorphology 71, 202–226.

Jochner, M., Turowski, J.M., Badoux, A., Stoffel, M., Rickli, C., 2015. The role of log jams and exceptional flood events in mobilizing coarse particulate organic matter in a steep headwater stream. Earth Surf. Dyn. 3 (3), 311–320. http://dx.doi.org/10. 5194/esurf-3-311-2015.

Kattelmann, R., 1997. Flooding from rain-on-snow events in the Sierra Nevada. Proc. Int. Assoc. Hydrol. Sci. 239, 59–65.

Keller, E.A., Swanson, F.J., 1979. Effects of large organic material on channel form and fluvial processes. Earth Surf. Process. 4, 361–380.

Kramer, N., Wohl, E., 2014. Estimating fluvial wood discharge using time-lapse photography with varying sampling intervals. Earth Surf. Process. Landf. 39 (6), 844–852. http://dx.doi.org/10.1002/esp.3540.

Latterell, J.J., Naiman, R.J., 2007. Sources and dynamics of large logs in a temperate floodplain river. Ecol. Appl. 17 (4), 1127–1141.

Macka, Z., Krejci, L., Louckova, B., Peterkova, L., 2011. A critical review of field techniques in the survey of large woody debris in river corridors: a central European perspective. Environ. Monit. Assess. 181, 291–316. http://dx.doi.org/10.1007/s10661-010-1830-8.

MacVicar, B.J., Piégay, H., 2012. Implementation and validation of video monitoring for wood budgeting in a wandering piedmont river, the Ain River (France). Earth Surf. Process. Landf. 37 (12), 1272–1289. http://dx.doi.org/10.1002/esp.1289.

MacVicar, B.J., Piégay, H., Henderson, A., Comiti, F., Oberlin, C., Pecorari, E., 2009. Quantifying the temporal dynamics of wood in large rivers: field trials of wood surveying, dating, tracking, and monitoring techniques. Earth Surf. Process. Landf. 34 (15), 2031–2046. http://dx.doi.org/10.1002/esp.1888.

Manners, R.B., Doyle, M.W., Small, M.J., 2007. Structure and hydraulics of natural woody debris jams. Water Resour. Res. 43, W06432. http://dx.doi.org/10.1029/ 2006WR004910.

Marcus, W.A., Rasmussen, J., Fonstad, M.A., 2011. Response of the fluvial wood system to fire and flood in Northern Yellowstone. Ann. Assoc. Am. Geogr. 101 (1), 21–44. http://dx.doi.org/10.1080/00045608.2010.539154.

Martin, D.J., Benda, L.E., 2001. Patterns of instream wood recruitment and transport at the watershed scale. Trans. Am. Fish. Soc. 130, 940–958.

McCabe, J.G., Clark, M.P., Hay, L.E., 2007. Rain-on-snow events in the western United States. Bull. Am. Meteorol. Soc. 319–328. http://dx.doi.org/10.1175/ BAMS-88-3-319.

Merten, E., Finlay, J., Johnson, L., Newman, R., Stefan, H., Vondracek, B., 2010. Factors influencing wood mobilization in streams. Water Resour. Res. 46, W10514. http://dx.doi.org/10.1029/2009WR008772.

Merz, J.E., Pasternack, G.B., Wheaton, J.M., 2006. Sediment budget for salmonid spawning habitat rehabilitation in a regulated river. Geomorphology 76, 207–228. http://dx.doi.org/10.1016/j.geomorph.2005.11.004.

Moulin, B., Piégay, H., 2004. Characteristics and temporal variability of large woody debris trapped in a reservoir on the River Rhone (Rhone): implications for river basin management. River Res. Appl. 20 (1), 79–97.

Mount, J.F., 1995. California Rivers and Streams: The Conflict Between Fluvial Processes and Land Use. University of California Press, Berkeley.

Ralph, F.M., Neiman, P.J., Wick, G.A., Gutman, S.I., Dettinger, M.D., Cayan, D.R., White, A.B., 2006. Flooding on California's Russian River: role of atmospheric rivers. Geophys. Res. Lett. 33, L13801. http://dx.doi.org/10.1029/2006GL026689.

Ruiz-Villanueva, V., Piégay, H., Gurnell, A., Marston, R.A., Stoffel, M., 2016. Recent advances quantifying large wood dynamics in river basins: new methods, remaining challenges. J. Geophys. http://dx.doi.org/10.1002/2015RG000514.

Schenk, E.R., Moulin, B., Hupp, C.R., Richter, J.M., 2014. Large wood budget and transport dynamics on a large river using radio telemetry. Earth Surf. Process. Landf. 39, 487–498. http://dx.doi.org/10.1002/esp.3463.

Seo, J.I., Nakamura, F., Nakano, D., Ichiyanagi, H., Chun, K.W., 2008. Factors controlling the fluvial export of large woody debris, and its contribution to organic carbon budgets at watershed scales. Water Resour. Res. 44, W04428. http://dx.doi. org/10.1029/2007WR006453.

Seo, J.I., Nakamura, F., Akasaka, T., Ichiyanagi, H., Chun, K.W., 2012. Large wood export regulated by the pattern and intensity of precipitation along a latitudinal gradient in the Japanese archipelago. Water Resour. Res. 48, W03510. http://dx.doi. org/10.1029/2011WR011880.

Seo, J.I., Nakamura, F., Chun, K.W., Kim, S.W., Grant, G.E., 2015. Precipitation patterns control the distribution and export of large wood at the catchment scale. Hydrol. Process. 29, 5044–5057. http://dx.doi.org/10.1002/hyp.10473.

Swanson, F.J., 2003. Wood in river: a landscape perspective. In: In: Gregory S.V, Boyer K.L. and Gurnell A.M., (Eds.), The Ecology and Management of Wood in World Rivers.

American Fisheries Society Symposium, 37. Bethesda, Maryland, pp. 299–313.

Swanson, F.J., Lienkaemper, G.W., Sedell, J.R., 1976. History, physical effects and management implications of large organic debris in western Oregon streams. In: USDA Forest Service General Technical Report PNW-56, Portland, Oregon.

Turowski, J.M., Badoux, A., Bunte, L., Rickli, C., Federspiel, N., Jochner, M., 2013. The mass distribution of coarse particulate organic matter exported from an Alpine headwater stream. Earth Surf. Dyn. 1, 1–11. http://dx.doi.org/10.5194/esurf-1-1-2013.

Vaughan, M.C., 2013. Large Streamwood Storage Does Not Decrease Downstream Through a Watershed (M.S. Thesis). University of California, Davis, California.

Veronique, B., Piégay, H., Buffin-Belanger, T., Vaudor, L., 2016. A new methodology for monitoring wood fluxes in rivers using a ground camera: potential and limits. Geomorphology. http://dx.doi.org/10.1016/j.geomorph.2016.07.019.

West, A.J., Lin, C.W., Lin, T.C., Hilton, R.G., Liu, S.H., Chang, C.T., Lin, K.C., Galy, A., Sparkes, R.B., Hovius, N., 2011. Mobilization and transport of coarse woody debris to the oceans triggered by an extreme tropical storm. Limnol. Oceanogr. 56, 77–85. http://dx.doi.org/10.4319/lo.2011.56.1.0077.

Wohl, E., 2016. Bridging the gap: an overview of wood across time and space in diverse rivers. Geomorphology. http://dx.doi.org/10.1016/j.geomorph.2016.04.014.

Wohl, E., Ogden, F.L., 2013. Organic carbon export in the form of wood during an

extreme tropical storm, Upper Rio Chagres, Panama. Earth Surf. Process. Landf. 38, 1407–1416. http://dx.doi.org/10.1002/esp.3389.
Wohl, E., Cenderelli, D.A., Dwire, K.A., Ryan-Burkett, S.E., Young, M.K., Fausch, K.D., 2010. Large in-stream wood studies: a call for common metrics. Earth Surf. Process. Landf. 35, 618–625. http://dx.doi.org/10.1002/esp.1966.
Yuba Salmon Partnership Initiative (YSPI), 2015. Term sheet for framework of settlement agreement, 18 p. http://www.dfg.ca.gov/fish/Resources/Chinook/YSPI/ (accessed May 28, 2015).